Thermodynamics of ammonia activation by iron cluster cations: Guided ion beam studies of the reactions of Fe_n^+ ($n=2-10,14$) with ND_3

Rohana Liyanage,[a] James B. Griffin, and P. B. Armentrout
Department of Chemistry, University of Utah, Salt Lake City, Utah 84112

(Received 23 May 2003; accepted 8 August 2003)

The kinetic energy dependences of the reactions of Fe_n^+ ($n=2-10,14$) with ND_3 are studied in a guided ion beam tandem mass spectrometer over the energy range of 0–10 eV. Dehydrogenation of ammonia to form Fe_nND^+ is found to be efficient and exothermic for $n=4$ in agreement with previous FT-ICR studies. In contrast to the ICR studies, we also observe exothermic dehydrogenation for $n=3$ and 5, although these processes are much less efficient than for $n=4$. Other clusters also undergo this process but exhibit an energy threshold. A multitude of other primary products are observed including $Fe_{n-1}ND_3^+$ ($n=2-4,9,10$), $Fe_nND_2^+$ ($n=1,4-8$), and $Fe_{n-1}ND_2^+$ ($n=2-5$), which all have reaction efficiencies that depend on cluster size. At high energies, Fe_nN^+ and Fe_nD^+ are observed along with products corresponding to Fe atom loss from the primary products. Thresholds for the various primary and secondary reactions are analyzed and bond energies for iron cluster cations bound to N, ND, ND_2, and ND_3 are determined. Comparisons of this thermochemistry to that for isoelectronic CD, CD_2, and CD_3 show that the binding of ND and ND_2 is enhanced by dative interactions of the lone pair of electrons with the cluster. In contrast, the N atom is found to have a weaker bond than CD for most cluster sizes. On the basis of this thermochemistry, we find that there are barriers to the dehydrogenation reactions of about 1 eV for all the clusters, except $n=3-5$ exhibit an additional low energy pathway. Bond energies for larger clusters are used to estimate the bond energies of the ND and ND_2 molecular fragments to iron surfaces. © *2003 American Institute of Physics.* [DOI: 10.1063/1.1614753]

I. INTRODUCTION

A principal motivation behind studies of the chemistry of gas-phase metal clusters is the idea that clusters may serve as models for surfaces and heterogeneous catalysts. Lending credence to this idea are the observations that many technologically important catalysts involve highly dispersed metals and that surface defect sites are often the active sites for chemistry.[1] Further, studies of gas-phase transition metal clusters find that as the cluster size increases, the chemistry rapidly reaches a limiting behavior, suggestive of an approach to bulk phase behavior. For example, previous work in our laboratory finds that average gas-phase cluster binding energies extrapolate nicely to the bulk-phase heat of vaporization as the cluster size increases.[2,3] Other studies find that the maximum binding energies of oxygen and deuterium atoms to modest-sized (>10 atoms) cationic clusters of V,[4,5] Cr,[6–8] Fe,[9–11] and Ni[12,13] are comparable to similar quantities for surfaces. Although such results were not necessarily anticipated, it does seem reasonable that the thermochemistry of clusters can be similar to that for bulk phase surfaces because chemical bonds are more local phenomena than quantities such as ionization energies and electron affinities.

Although more extensive research is required for both clusters and surfaces in order to determine how accurate this cluster-surface analogy might be, an intriguing possibility is that the analogy will actually fail for at least some clusters, i.e., specific-sized clusters may be found with very high chemical specificity. One interesting example of a cluster showing unique reactivity is Fe_4^+. Irion and co-workers found that Fe_4^+ is unique in its ability to form benzene from smaller hydrocarbons[14] and in its thermal reactivity with ammonia[15] and ethane.[16] In their study of the ammonia system,[15] the iron cluster ions were generated by sputtering with 20 keV Xe ions and then trapped, collisionally thermalized, and isolated in an ion cyclotron resonance (ICR) mass spectrometer. These thermalized clusters were exposed to ammonia at roughly 5×10^{-8} mbar and reactions at room temperature were studied. No reaction was found for iron dimer and trimer ions and Fe_5^+ through Fe_{13}^+ slowly adsorbed intact NH_3 molecules. According to these studies, the only species exhibiting enhanced reactivity was the tetramer, which dehydrogenates NH_3 to yield Fe_4NH^+ as the only primary reaction observed. Sequential reactions with additional ammonia molecules lead to $Fe_4(NH)_2^+$, $Fe_4(NH)_2(NH_3)^+$, and $Fe_3(NH)_2(NH_3)^+$, showing the presence of more active sites in the cluster. No quantitative reaction rates were reported for any of the processes observed. Very recently, Fossan and Uggerud have repeated these thermal energy studies again using ICR and clusters formed in a pulsed laser vaporization/supersonic expansion source.[17] Qualitatively, these authors obtained the same results as the previous ICR studies but report quantitative reaction rates, which reach maxima for $n=4$, 12, and 19 and minima for $n=6$ and 17. In addition, they examine the reac-

[a]Present address: Statewide Mass Spectrometry Facility, University of Arkansas, Fayetteville, AR 72701.

tions of Fe_4NH^+ and $Fe_nNH_3^+$ ($n=5-18$) with NH_3 and several other related reactions.

Experimentally, the interaction of ammonia on iron surfaces has been studied extensively in order to understand the catalytic synthesis of ammonia from N_2 and H_2, the Haber process.[18] The industrial catalyst is iron oxide with small amounts of Al_2O_3 and K_2O and sometimes other oxides added. Detailed studies of the relevant reactions on iron surfaces indicate that the rate-limiting step to ammonia synthesis is N_2 activation, which has a barrier that is reduced by the potassium promoter. Ammonia is known to adsorb to iron surfaces nondissociatively at low temperatures, whereas at higher energies, stepwise dissociation occurs yielding a stable adsorbed NH intermediate. Energetics for the various intermediates, H, N, NH, NH_2, and NH_3, adsorbed to iron surfaces have been estimated.[18]

In the present work, we examine the reactions of size-specific iron cluster cations with ammonia using guided ion beam tandem mass spectrometry. We are able to examine the kinetic energy dependence of these reactions from the thermal energies accessible in the ICR studies to approximately 10 eV. The sensitivity of the method allows us to verify the qualitative conclusions of Schnabel and Irion[15] regarding the unusual reactivity of Fe_4^+, however, we demonstrate that other clusters also react similarly with ammonia. Sequential processes are not accessible in the present work, because our experiments are done under single collision conditions. The results are interpreted to yield thermodynamic information about a number of products observed in these processes as a function of cluster size. We present qualitative explanations for the bond energies obtained for $Fe_n^+-ND_x$ and size-specific cluster reactivities using simple molecular orbital arguments.

II. EXPERIMENT

The ion beam apparatus and experimental techniques used in this work have been described in detail elsewhere.[19] A brief description is given here. Iron cluster ions are formed by laser vaporization/supersonic expansion.[20] The output of an Oxford ACL 35 copper vapor laser operating at 7–8 kHz is tightly focused onto a continuously translating and rotating iron target rod (cold-rolled steel) inside an aluminum source block.[21] The optimum pulse energy for iron cluster ion production ranges between 3 and 4 mJ/pulse. The vaporized material is entrained in a continuous flow ($5-6\times10^3$ sccm) of He passing over the ablation surface. Frequent collisions and rapid mixing leads to the formation of thermalized clusters as they travel down a 2 mm diameter×63 mm long condensation tube. Although direct measurements of the internal temperatures of the clusters are not possible, previous studies have indicated that the clusters are not internally excited and likely to be near room temperature.[25]

This seeded helium flow then undergoes a mild supersonic expansion in a field free region and is skimmed. Positively charged ions are focused through two differentially pumped regions, accelerated, and injected into a 60° magnetic sector momentum analyzer. The mass selected ions are decelerated and focused into an octopole ion guide[22] that extends through a reaction cell. The octopole beam guide is biased with dc and rf voltages. The former allows us to accurately control the translational energy of the incoming ions, whereas the latter establishes a radial potential that efficiently traps the reactant and product ions that travel through the octopole. The pressure of ND_3 neutral reactant gas (99.8% purity) in the reaction cell is kept relatively low to reduce the probability of multiple collisions with the ions. All studies were conducted at $1-5\times10^{-4}$ mbar ND_3 pressures. The resultant cross sections show no pressure dependence for all cluster sizes and products except for the $Fe_nND_3^+$ adducts. For these latter products, the cross sections are extrapolated to zero reactant pressure such that all cross sections presented here are the result of single ion-molecule collisions. The product and reactant ions drift to the end of the octopole, where they are extracted, and injected into a quadrupole mass filter for mass analysis. Ion intensities are measured with a Daly detector[23] coupled with standard pulse counting techniques. Reactant ion intensities used in these studies ranged from $0.5-1.0\times10^6$ ions/s. Observed product intensities are converted to absolute reaction cross sections as discussed in detail elsewhere.[24] Absolute errors in the cross sections are on the order of ±30%.

Results for each reaction system were repeated several times to ensure their reproducibility. CID experiments with Xe were performed on all the cluster ions to ensure their identity and the absence of any excessive internal excitation. In all instances, CID thresholds are consistent with those previously reported.[25] The absolute zero in the kinetic energy of the ions and their energy distributions (the latter varying from 0.7–2 eV) were measured using the octopole as a retarding energy analyzer.[24] The error associated with the absolute energy scale is 0.05 eV in the lab frame. Kinetic energies in the laboratory frame are converted to center-of-mass (CM) energies using the stationary target approximation, $E(\mathrm{CM})=E(\mathrm{lab})m/(m+M)$ where m and M are the masses of the neutral and ionic reactants, respectively. The data at the lowest energies are corrected for truncation of the ion beam energy distribution.[24]

The products observed in this work include $Fe_nND_x^+$ and Fe_nD^+ species where $x=0-3$. Accurate measurements of the intensities of these species depend on our ability to resolve and transport them efficiently to the detector. Resolving the high intensity Fe_n^+ reactant ions from the low intensity Fe_nD^+ product ions proved to be difficult even when the quadrupole mass analyzer is set to operate at high resolution. In principle, the resolution could be increased sufficiently to separate the parent and product ions, but as this limit is approached, the transmission of the ions is reduced to the extent that the experiments become impractical and inaccurate. Therefore the experiments are conducted by adjusting the resolution of the quadrupole mass filter to be as high as possible without reducing the product ion intensities. Mass overlap of product ions differing by two and four mass units is easily identified when the energy dependence of their cross sections differ. When product ions have similar energy dependences, we estimate the mass overlap by measuring the intensity of the intense reactant beam at two and four mass

units above and below the peak intensity. This procedure also helps in the analysis of any mass overlap between $Fe_nND_x^+$ product ions. Cross sections shown below have been corrected for such overlap in all cases where the correction is unambiguous. It is possible that some residual intensity resulting from mass overlap remains.

III. RESULTS

In all systems, reactions of iron cluster cations with $d3$-ammonia were conducted from thermal energies to 10 eV in the center-of-mass frame. Fe_n^+ reactant clusters ranging in size from $n=1-10$ and 14 were studied. ND_3 was used instead of NH_3 because this enhances the mass separation between products. (The exothermic reactions of the $n=3-5$ clusters with NH_3 were studied and the results were the same as for ND_3 within experimental error.) In the discussion that follows, results for the smaller clusters are examined in detail, followed by an overview of those for larger clusters. To calculate reaction efficiencies at low energies, the absolute cross sections are compared with those calculated using the trajectory results of Su,[26] in which the polarizability of ammonia is taken as 2.16 $Å^3$ and the dipole moment is 1.47 D.[27]

To help organize the results of the myriad reactions observed, we first note which processes are possible and observed in at least one of the cluster systems. These can be grouped into reactions in which no loss of iron atoms occurs, processes (1)–(5),

$$Fe_n^+ + ND_3 \rightarrow Fe_nD^+ + ND_2, \quad (1)$$

$$\rightarrow Fe_nND_2^+ + D, \quad (2)$$

$$\rightarrow Fe_nND^+ + D_2, \quad (3)$$

$$\rightarrow Fe_nN^+ + D + D_2, \quad (4)$$

$$\rightarrow Fe_nND_3^+. \quad (5)$$

At lower energies, the exchange of neutral iron atom with ammonia takes place according to reactions (6),

$$Fe_n^+ + ND_3 \rightarrow Fe_{n-1}ND_3^+ + Fe. \quad (6)$$

At higher energies, products with fewer iron atoms are formed in the simple collision-induced dissociation reactions (7a),

$$Fe_n^+ + ND_3 \rightarrow Fe_{n-1}^+ + Fe + ND_3, \quad (7a)$$

although we also find evidence for processes (7b),

$$Fe_n^+ + ND_3 \rightarrow Fe_{n-1}^+ + FeND_3, \quad (7b)$$

which produces the same ionic products. Additional products having fewer iron atoms are formed in dissociations of the products formed in reactions (1)–(5). Reactions (8)–(13) comprise the latter types of processes observed,

$$\rightarrow Fe_{n-1}D^+ + Fe + ND_2, \quad (8)$$

$$\rightarrow Fe_{n-1}ND_2^+ + FeD, \quad (9a)$$

$$\rightarrow Fe_{n-1}ND_2^+ + Fe + D, \quad (9b)$$

$$\rightarrow Fe_{n-1}ND^+ + Fe + D_2, \quad (10)$$

$$\rightarrow Fe_{n-1}N^+ + Fe + D + D_2, \quad (11)$$

$$\rightarrow Fe_{n-2}ND_3^+ + 2Fe, \quad (12)$$

$$\rightarrow Fe_{n-2}ND^+ + 2Fe + D_2. \quad (13)$$

In most cases, the identity of the concomitant neutral products is obvious, but in reaction (9), evidence for two pathways is observed as discussed below. Because of the many products observed, plots for each cluster system are broken down into two separate parts for clarity: part a shows cross sections for reactions (1)–(5) and part b shows cross sections for reactions (7)–(13).

A. $Fe^+ + ND_3$

Previous experiments[28] in our lab have shown that the laser vaporization source generates atomic iron ions primarily in their ground ^6D state with about 3% of the ions in the ^4F first excited electronic state at 0.23 eV. These iron monomer ions react with ND_3 to form only FeD^+ and $FeND_2^+$ in reactions (1) and (2), both of which are considerably endothermic. A more extensive study of this system in which variations of the ion source are used to systematically alter the state distribution provides state-specific results for reaction of ground state $Fe^+(^6D)$ and excited state $Fe^+(^4F)$.[29] This study shows that the latter state is much more reactive (by over a factor of 20).

B. $Fe_2^+ + ND_3$

Addition of a second Fe atom to the reactant cluster ion greatly increases the reactivity of the cluster and the complexity of the reaction, Fig. 1. A number of different products are observed in reactions (1), (3), (4), (6)–(9). $FeND_3^+$ is formed at low energies in process (6), which corresponds to displacement of an iron atom by ND_3. The reaction is endothermic, Fig. 1(b), which is consistent with previously measured thermochemistry, $D_0(Fe^+-Fe)=2.74\pm0.10$ eV,[25] and $D(Fe^+-NH_3)=1.90\pm0.12$ eV.[30] The $FeND_3^+$ product has a cross section that reaches a maximum of 1 $Å^2$ at about 1 eV and then declines rapidly. None of the other products observed have cross sections that are sufficiently large to account for the sharp decline in the $FeND_3^+$ product cross section, which indicates that this product disappears because the $Fe_2ND_3^+$ precursor decomposes preferentially by ammonia loss with an increasingly shorter lifetime as energy is increased.

The apparent threshold for Fe^+ production is about 1 eV lower than the thermodynamic threshold for the simple dimer dissociation reaction (7a), 2.74±0.10 eV, Fig. 1(b). Hence formation of Fe^+ at threshold must correspond to reaction (7b) where the $FeND_3$ neutral is formed instead of Fe and ND_3. At higher energies, simple CID almost certainly contributes to the observed Fe^+ cross section. Fe_2ND^+ is also produced at relatively low energies in the dehydrogenation reaction (3). Fe_2N^+ is produced by the loss of D atom from the Fe_2ND^+, although it is possible that a $Fe_2ND_2^+$ precursor has a cross section too small to observe (consistent with the relative magnitudes of the analogous Fe_nD^+ versus $Fe_nND_2^+$ cross sections for the trimer, next section). The sum of the Fe_2ND^+ and Fe_2N^+ product cross sections declines as

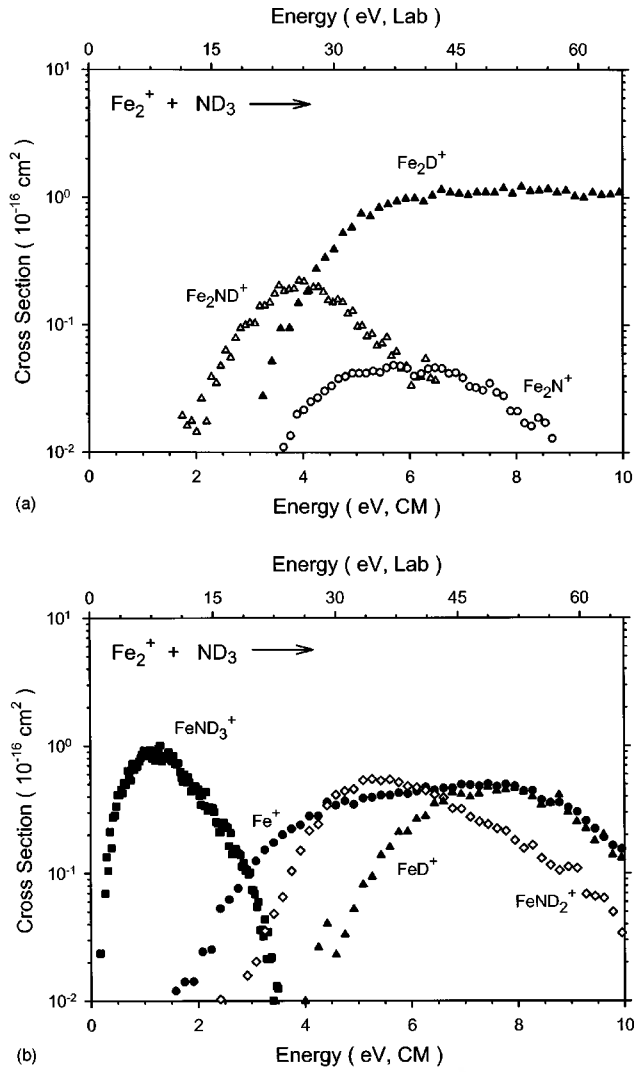

FIG. 1. Product cross sections for the reaction of Fe_2^+ with ND_3 as a function of collision energy in the center of mass (lower x-axis) and laboratory axis (upper x-axis). Parts (a) and (b) show Fe_2L^+ and FeL^+ cross sections, respectively.

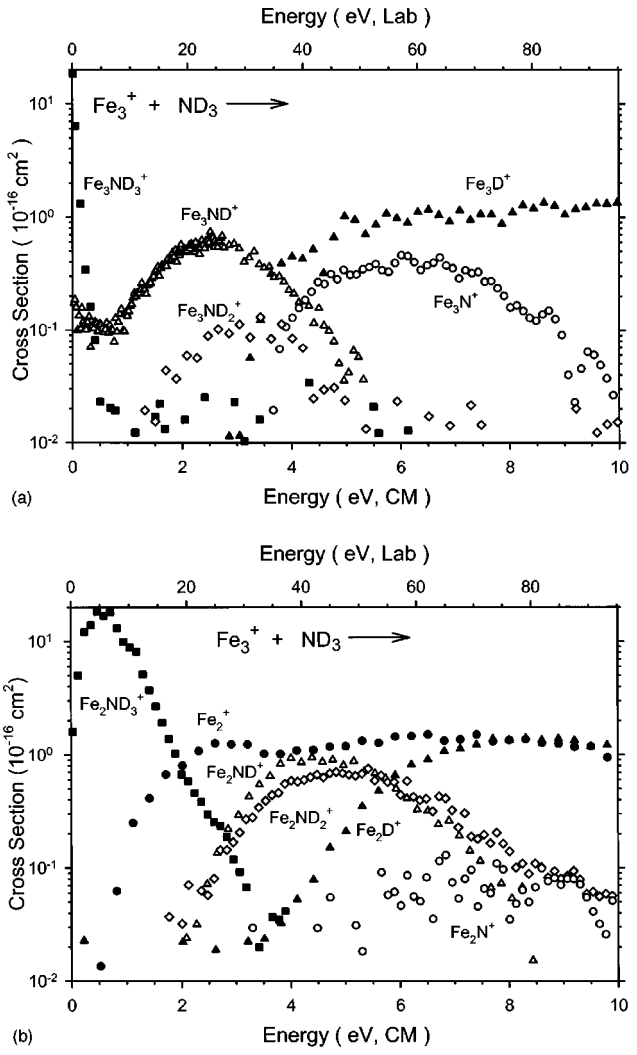

FIG. 2. Product cross sections for the reaction of Fe_3^+ with ND_3 as a function of collision energy in the center of mass (lower x-axis) and laboratory axis (upper x-axis). Parts (a) and (b) show Fe_3L^+ and Fe_2L^+ cross sections, respectively.

the Fe_2D^+ product channel increases. This behavior suggests that formation of Fe_2ND^+ and Fe_2D^+ compete with each other and share a common intermediate, presumably the chemisorbed $DFe_2ND_2^+$ species for reasons discussed below. The $FeND_2^+$ product can be formed by losing FeD from the intermediate $DFe_2ND_2^+$, reaction (9b), by losing a D atom from $FeND_3^+$, reaction (9a), or by losing an Fe atom from $Fe_2ND_2^+$. This latter mechanism is unlikely for the dimer because we do not observe a $Fe_2ND_2^+$ product. Because the $FeND_3^+$ product is nearly gone by the threshold for $FeND_2^+$, reaction (9b) is also unlikely. Therefore, production of $FeND_2^+$ is assigned to reaction (9a), a mechanism supported by the energetics, which are discussed below. The other product formed at high energies, FeD^+, is the result of reaction (8), which occurs by Fe atom loss from the primary Fe_2D^+ product ion.

C. $Fe_3^+ + ND_3$

Key differences in the reactivity of the iron trimer cation with ND_3 compared to the dimer are the observation of adduct formation; $Fe_3ND_3^+$ formed in reaction (5), and the observation that the dehydrogenation process, reaction (3), has a small exothermic component, Fig. 2. Compared to the collision rate, the $Fe_3ND_3^+$ species is formed with about a 3% efficiency at the lowest energies (0.012 eV) and then falls off rapidly with increasing energy. This decline is apparently a result of Fe atom loss, leading to $Fe_2ND_3^+$ in reaction (6), which has a comparable maximum magnitude as the $Fe_3ND_3^+$ product. This reaction is clearly less endothermic than the equivalent process in the dimer system, consistent with the lower bond energy of the iron trimer cation, $D_0(Fe_2^+-Fe) = 1.67 \pm 0.12$ eV.[25] The structure of these species is not clear. It is possible that these products correspond to ammonia physisorbed to the cluster ion, but dissociative chemisorption is also possible and suggested by the ND bond activation processes. It does seem odd that a physisorbed species would prefer to dissociate by losing an Fe atom even though loss of the ammonia is thermodynamically favored. This preference suggests that the $Fe_3ND_3^+$ and $Fe_2ND_3^+$ species may have activated the ND bond. Note that a phys-

isorbed adduct could be stabilized by additional collisions with ND_3, but the cross section shown has been extrapolated to zero pressure of ND_3, eliminating the contributions of collisional stabilization.

The observation of exothermic dehydrogenation, Fig. 2, contrasts with the fact that neither Irion and Schnabel[15] nor Fossan and Uggerud[17] reported this reaction in their ICR studies of iron cluster ions with ammonia. In our results, we find that this reaction occurs at only 0.1% of the collision rate, suggesting that the ICR work may not have adequate sensitivity to observe this reaction. Alternatively, the different methods of cluster generation and isolation may lead to different results, with our system more likely to produce truly thermal cluster ions. The dehydrogenation product, Fe_3ND^+, dissociates mainly by losing an Fe atom to form Fe_2ND^+. Fe_3ND^+ can also dissociate by losing a D atom to form Fe_3N^+, which could also be produced by losing D_2 from $Fe_3ND_2^+$. Similar to the dimer, formation of the dehydrogenation product, Fe_3ND^+, appears to compete with generation of the cluster deuteride, Fe_3D^+, which is the only channel large enough to explain the decline in the sum of the Fe_3ND^+, Fe_2ND^+, and Fe_3N^+ products. Small amounts of $Fe_3ND_2^+$ formed in reaction (2) are also observed. The cross section for this product is small because formation of $Fe_3ND_2^+$ competes with formation of Fe_3D^+ and Fe_3ND^+ products, and angular momentum constraints heavily favor Fe_3D^+ formation over $Fe_3ND_2^+$.[31–33] Other products observed for the trimer reaction with ammonia result from sequential loss of D atoms or Fe atoms from their primary counterpart. Fe_2D^+ is produced by loss of Fe atom from Fe_3D^+. Fe_2N^+ could be produced by losing Fe from Fe_3N^+, D from Fe_2ND^+, or D_2 from $Fe_2ND_2^+$, but a dominant process is not clear from the cross sections. $Fe_2ND_2^+$ can be produced by loss of FeD from the $DFe_3ND_2^+$ intermediate via reaction (9a), loss of a D atom from $Fe_2ND_3^+$, or loss of Fe from $Fe_3ND_2^+$. At threshold, the former process is indicated by thermodynamic arguments discussed below, although the other pathways probably contribute at higher energies.

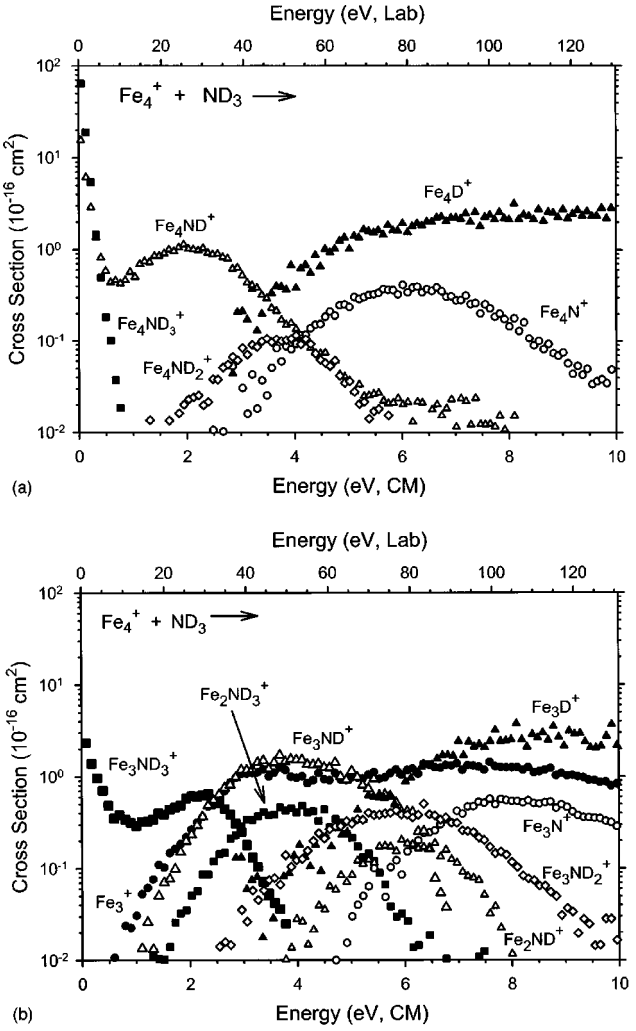

FIG. 3. Product cross sections for the reaction of Fe_4^+ with ND_3 as a function of collision energy in the center of mass (lower x-axis) and laboratory axis (upper x-axis). Parts (a) and (b) show cross sections for Fe_4L^+ and for fragments having fewer iron atoms, respectively.

D. $Fe_4^+ + ND_3$

In our work, the iron tetramer cation is observed to undergo three reactions at thermal energies, Fig. 3. The dominant process is adduct formation in reaction (5), which occurs at about 20% of the collision rate. The tetramer also undergoes the dehydrogenation reaction to form Fe_4ND^+, reaction (3), much more efficiently (about 5% of the collision rate) than the trimer (0.1%), but also shows two features, as does the trimer. The exchange reaction (6) is also exothermic and exhibits two features. It is found to have a reaction efficiency at thermal energies of about 1% of the collision rate. Irion and Schnabel[15] and Fossan and Uggerud[17] observed the dehydrogenation process as the only exothermic reaction in their ICR studies, and did not observe adduct formation, which we find is even more efficient. Fossan and Uggerud find that reaction (3) occurs with an efficiency of 12%, compared to our value of 5% for reaction (3) and 26% for all processes. The most likely explanation for these differences is the timescale of the experiments. In our studies, ions are observed after a flight time of $\sim 10^{-4}$ s, such that some $Fe_4ND_3^+$ intermediates can be observed, whereas at the longer timescale of the ICR experiments (seconds), such intermediates have more time to form Fe_4ND^+ products or reform reactants.

At higher energies, Fe_3^+ is observed but with a threshold about 1 eV below that for simple CID, reaction (7a). This indicates that reaction (7b) must be occurring with contributions from CID starting at higher energies. Fe_4ND^+ dissociates mainly by losing an iron atom, as indicated by a smooth energy dependence in the sum of the cross sections of Fe_4ND^+ and Fe_3ND^+. Likewise, the sum of the cross sections of $Fe_4ND_2^+$ and $Fe_3ND_2^+$ has a smooth energy dependence, suggesting that $Fe_3ND_2^+$ is produced mainly by losing an iron atom from $Fe_4ND_2^+$ rather than losing a D atom from $Fe_3ND_3^+$ or FeD from $Fe_4ND_3^+$. Note that this conclusion indicates that reaction (9a) is not observed in the tetramer system, in contrast to the dimer and trimer systems; a result that can be verified by the thermodynamics (see below). Fe_4N^+ is produced either by losing a D atom from Fe_4ND^+

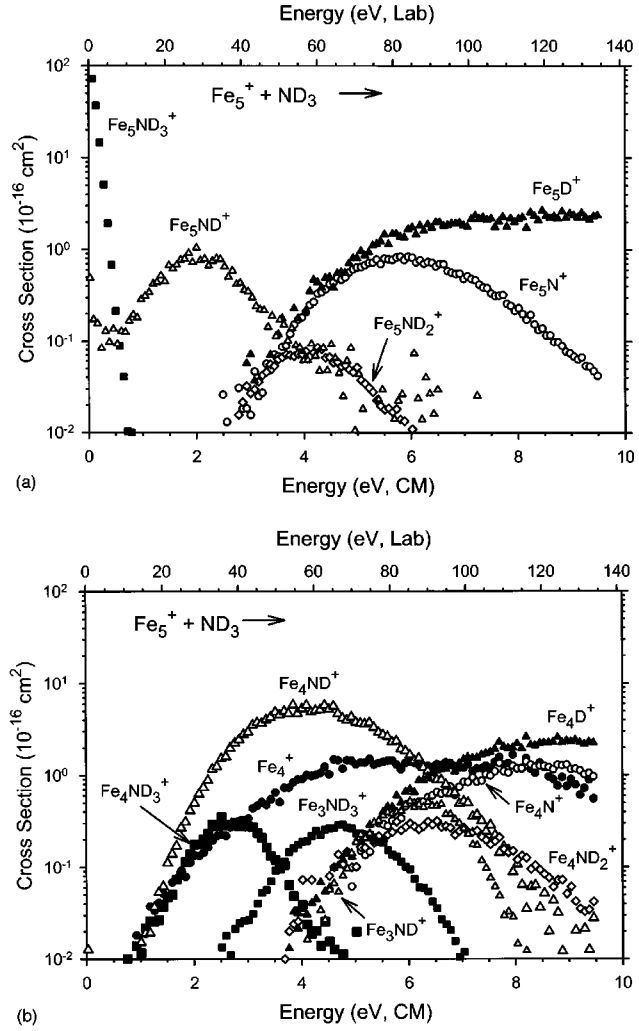

FIG. 4. Product cross sections for the reaction of Fe_5^+ with ND_3 as a function of collision energy in the center of mass (lower x-axis) and laboratory axis (upper x-axis). Parts (a) and (b) show cross sections for Fe_5L^+ and for fragments having fewer iron atoms, respectively.

or by eliminating D_2 from $Fe_4ND_2^+$, but the relative energy dependences of these cross sections appear more consistent with the latter. Similarly, Fe_3N^+ can be produced either by losing an iron atom from Fe_4N^+ or D_2 from $Fe_3ND_2^+$, rather than losing a D atom from Fe_3ND^+. The iron tetramer cation also produces two tertiary products, $Fe_2ND_3^+$ and Fe_2ND^+, formed by losing an Fe atom from the corresponding secondary products, $Fe_3ND_3^+$ and Fe_3ND^+, via reactions (12) and (13).

E. $Fe_5^+ + ND_3$

As observed by Irion and Schnabel[15] and Fossan and Uggerud,[17] the dominant reaction of the iron pentamer cation with ammonia is adduct formation, reaction (5), Fig. 4, which we find occurs at about 30% of the collision rate at thermal energies, slightly higher than the efficiency for the tetramer. Fossan and Uggerud find an efficiency of only 2%, which presumably indicates that the $Fe_5ND_3^+$ species decomposes back to reactants given more time. Both ICR studies report reaction (5) as the only thermal reaction, whereas we find that the pentamer also undergoes the dehydrogenation reaction (3), similar to the trimer and tetramer. However, the reaction efficiency is much less than the tetramer, only 0.1% of the collision rate at thermal energies. As for the trimer and tetramer, the pentamer also exhibits an endothermic feature in the dehydrogenation reaction. Unlike the tetramer, the pentamer does not undergo the exchange reaction (6) until much higher energies (apparent threshold of about 1 eV).

The $Fe_5ND_3^+$ product disappears rapidly with increasing energy such that it must dissociate by returning to reactants (loss of ND_3). We do observe $Fe_4ND_3^+$ at higher energies, however, which must come from Fe loss from the transiently formed $Fe_5ND_3^+$. It seems plausible that this alternate decomposition pathway might happen preferentially for complexes where dissociative chemisorption to form $DFe_5ND_2^+$ has occurred. Formation of Fe_4^+ has a threshold below $D_0(Fe_4^+ - Fe) = 2.53 \pm 0.23$ eV,[25] indicating that reaction (7b) must be occurring at low energies, whereas reaction (7a) certainly contributes at higher energies. Similar to the analogous product in the trimer and tetramer systems, Fe_5ND^+ dissociates mainly by loss of an iron atom to yield Fe_4ND^+, which in turn loses Fe to form Fe_3ND^+. The decline in the sum of the Fe_nND^+ products ($n = 3-5$) correlates with the increase in the Fe_nD^+ product cross sections, illustrating that these products are coupled. Fe_5N^+ is probably produced primarily by loss of D_2 from $Fe_5ND_2^+$ although loss of a D atom from Fe_5ND^+ may also contribute. Higher energy products are produced by sequential loss of Fe atoms from precursors Fe_4ND^+, $Fe_4ND_3^+$, $Fe_5ND_2^+$, Fe_5N^+, and Fe_5D^+. Alternate pathways may also contribute.

F. Fe_n^+ ($n = 6-10,14$) + ND_3

Figure 5 shows product cross sections for reaction of the iron hexamer cation with ammonia and is representative of all larger clusters. Detailed results for Fe_n^+ ($n = 7-10,14$) are provided as Figs. 1S–5S in the supplementary material.[42] Because the overall chemistry does not change appreciably for larger clusters, Fe_{14}^+ was chosen as representative of the behavior of the larger clusters and no studies of the $n = 11-13$ clusters were performed. The dominant reaction in all cases studied at thermal energies is adduct formation, in agreement with the observations of Irion and Schnabel[15] and Fossan and Uggerud.[17] As shown in Fig. 6, the efficiencies of these reactions gradually increase with cluster size from about 45% for $n = 6$ and 7 to about 75% for $n = 8-10$ and 14. These rates are considerably higher than those of Fossan and Uggerud[17] who found a maximum rate (among the clusters studied here) in the cases of $n = 4$ and 14, which is only 12%–14% of the collision rate, and a minimum rate for $n = 6$ of 1%. This difference can be attributed to the timescales for the two measurements, 10^{-4} s here and seconds in the ICR experiments, and indicates that the $Fe_nND_3^+$ species observed here are metastable.

The kinetic energy at which the $Fe_nND_3^+$ product cross section declines increases by almost 1 eV over this range of cluster sizes, Fig. 6. At higher energies, the dehydrogenation reaction (3) is a dominant process and exhibits a threshold in all cases, Fig. 5. The Fe_nND^+ species dissociates predom-

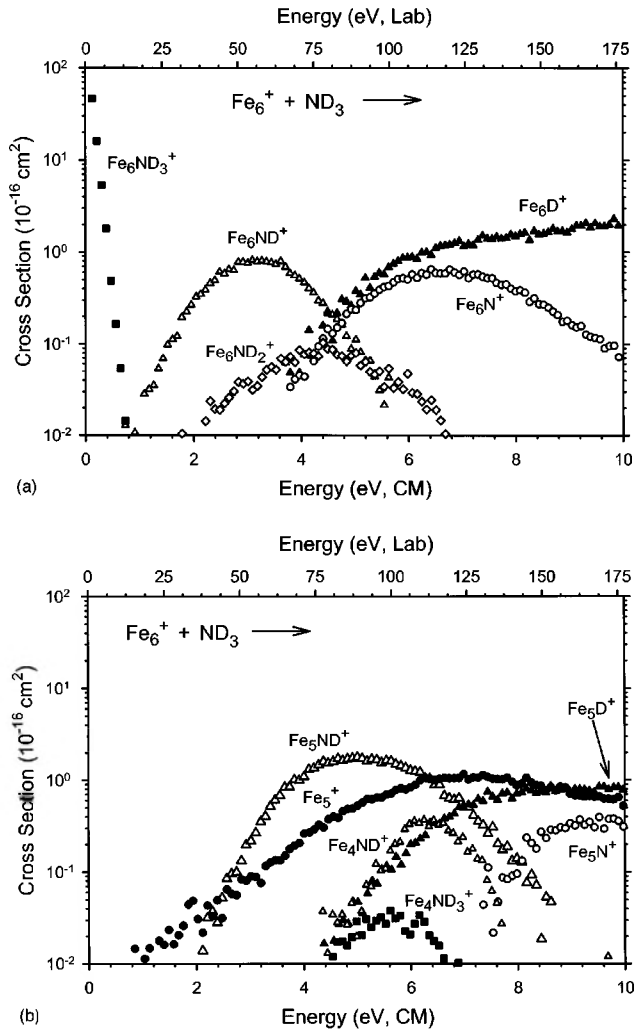

FIG. 5. Product cross sections for the reaction of Fe_6^+ with ND_3 as a function of collision energy in the center of mass (lower x-axis) and laboratory axis (upper x-axis). Parts (a) and (b) show cross sections for Fe_6L^+ and for fragments having fewer iron atoms, respectively.

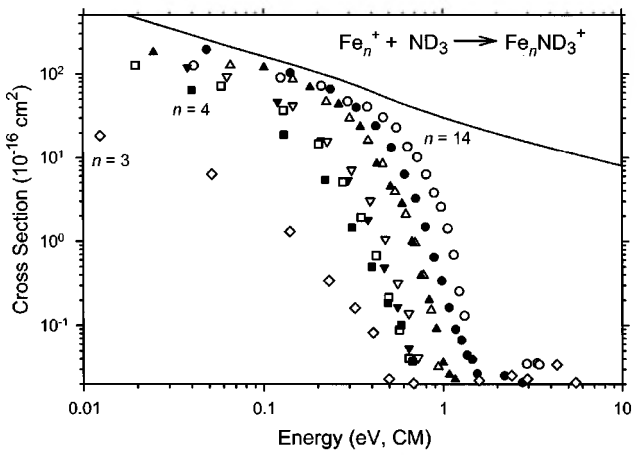

FIG. 6. Product cross sections for reaction (5) as a function of collision energy in the center of mass (lower x-axis). Data are shown for $n=3$ (open diamond), 4 (closed square), 5 (open square), 6 (inverted closed triangle), 7 (inverted open triangle), 8 (closed triangle), 9 (open triangle), 10 (closed circle), and 14 (open circle). The full line shows the collision cross section from trajectory calculations (see text).

inantly by Fe atom loss. Competition with Fe_nD^+ is also observed as are small amounts of $Fe_nND_2^+$, which appears to lose D_2 to yield Fe_nN^+. (No cross section for the $Fe_nND_2^+$ product is reported for $n=9$, 10, and 14 because this small intensity product becomes more difficult to resolve from the much more intense Fe_nND^+ product at these high masses.) Each of these products dissociates by iron atom loss at higher energies, although the $Fe_{n-1}ND_2^+$ is generally too small to see. We also observe the Fe_{n-1}^+ products, which have apparent thresholds generally lying below the threshold for reaction (7a) such that a small contribution from reaction (7b) is likely in all cases. The exchange reaction (6) is absent for the 6, 7, and 8 mers (in all cases, these products were explicitly looked for but not found, conservatively indicating that they have cross sections less than 10^{-17} cm^2), but reappears for the 9 and 10 mers. Oddly, reaction (12), which involves the loss of two iron atoms to form $Fe_{n-2}ND_3^+$, is observed for the 6–8 mers, but not larger clusters. Apparently, the magnitude of these products is affected by the size of the cluster, which affects the ability to dissipate excess energy, thereby influencing the lifetime of the adduct. Thus, the smaller clusters need to lose two iron atoms to stabilize a $Fe_xND_3^+$ species, whereas the larger clusters apparently have sufficiently long lifetimes to be observed after losing only one Fe atom. Such factors apparently influence the likelihood of observing reactions (13) for the largest clusters ($n=9$, 10, and 14) as well.

IV. THRESHOLD ANALYSIS AND THERMOCHEMISTRY

A. Data analysis

The energy dependences of cross sections for endothermic processes in the threshold region are modeled using Eq. (14),

$$\sigma(E)=\sigma_0\sum g_i(E+E_i-E_0)^N/E, \tag{14}$$

where σ_0 is an energy independent scaling parameter, N is an adjustable parameter, E is the relative kinetic energy, and E_0 is the threshold for reaction at 0 K. The summation is over the rovibrational states of the clusters having energies E_i and populations g_i where $\Sigma\, g_i=1$. Details about our implementation of this equation are given elsewhere.[34–36] Briefly, the Beyer-Swinehart algorithm[37,38] is used to evaluate the density of the ion rovibrational states, and then the relative populations, g_i, are calculated by the appropriate Maxwell-Boltzmann distribution at 300 K. Vibrational frequencies for the bare metal clusters are obtained by using an elastic model proposed by Shvartzburgh *et al.*[39] Before comparison with the data, this model cross section is also convoluted with the kinetic energy distributions of the ion and neutral reactants.[24]

For metal clusters, it has been shown that lifetime effects become increasingly important as the size of the cluster increases. This is because metal clusters have many low frequency vibrational modes such that the lifetime of the transient intermediate can exceed the experimental time available for reaction (approximately 10^{-4} s in our apparatus). Thus, an important component of the modeling of these reactions is to include the lifetime of the reaction, as esti-

mated using statistical Rice-Ramsperger-Kassel-Marcus (RRKM) theory.[38,40,41] The means to do this has been discussed in detail previously[34] and requires molecular constants for the energized molecule (EM) and transition state (TS) leading to the product of interest. The molecular constants used for the EMs and TSs for all reactions are provided along with detailed explanations for their choices in Ref. 42. Optimized fitting parameters of Eq. (14) for the analyses of all reaction cross sections ($n=2-10$ and 14) are given in Ref. 42 as Tables S2–S11, respectively.

B. Primary, secondary, and tertiary reactions

A fortunate aspect of cluster studies is the observation of identical product ions formed in primary, secondary, and tertiary reactions. Thus, a species like Fe_nL^+ may be formed as a primary product in the reaction of Fe_n^+ with ammonia, reaction (15), a secondary product of the reaction of Fe_{n+1}^+ with ammonia, reactions (16) or (17), and a tertiary product of the reaction of Fe_{n+2}^+ with ammonia, reaction (18).

$$Fe_n^+ + ND_3 \rightarrow Fe_nL^+ + (ND_3-L), \quad (15)$$

$$Fe_{n+1}^+ + ND_3 \rightarrow Fe_nL^+ + Fe + (ND_3-L), \quad (16)$$

$$Fe_{n+1}^+ + ND_3 \rightarrow Fe_nL^+ + Fe(ND_3-L), \quad (17)$$

$$Fe_{n+2}^+ + ND_3 \rightarrow Fe_nL^+ + 2Fe + (ND_3-L). \quad (18)$$

Hence, we have up to four independent means of determining the thermochemistry of the Fe_nL^+ products. It is conceivable that thresholds obtained for the secondary (16) and tertiary (18) reactions could be higher than thermodynamic values, if the total energy available is not efficiently retained by $Fe_{n+1}L^+$ precursors. However, if we assume the energy is divided among the products statistically, we can expect that the $Fe_{n+1}L^+$ products will retain much more energy than the Fe and ND_3-L products, which have many fewer degrees of freedom. Similar considerations hold for alternate mechanistic pathways for the secondary reactions. Clearly, this assumption could degrade for the smallest clusters and we explicitly consider this question below. Similar considerations were also explored in our recent studies on $Fe_n^+ + CD_4$ and there the comparison of bond energies obtained from the primary and secondary processes showed the basic validity of these assumptions.[43]

Optimized modeling parameters of Eq. (14) for all reactions are given in Tables S2–S11 of the supplementary material.[42] The threshold energies listed there for reactions (15)–(18) can be converted to bond energies of interest using Eqs. (19)–(22),

$$D(Fe_n^+-L) = D(ND_3-L) - E_0(15), \quad (19)$$

$$D(Fe_n^+-L) = D(ND_3-L) + D(Fe_n^+-Fe) - E_0(16), \quad (20)$$

$$D(Fe_n^+-L) = D(ND_3-L) + D(Fe_n^+-Fe) - E_0(17) - D[Fe-(ND_3-L)], \quad (21)$$

$$D(Fe_n^+-L) = D(ND_3-L) + D(Fe_{n+1}^+-Fe) + D(Fe_n^+-Fe) - E_0(18), \quad (22)$$

where $D(ND_3-L)$ is the energy required to remove L from ND_3. In Eqs. (20), (21), and (22), the dissociation energies for the bare Fe_n^+ clusters are taken from previous studies in our laboratory.[25] In the present work, neutral $Fe(ND_3-L)$ species observed include only FeD and $FeND_3$. The bond energy for the former is 1.49 ± 0.04 eV[44,45] and the latter is derived here.

TABLE I. Fe_n^+-D bond energies (eV) obtained from the literature and analyses of reactions (1) and (8).

	Fe_n^+-D[a]	Fe_n^+-D (1)[b]	Fe_n^+-D (8)[c]
1	2.16±0.06		2.35±0.23
2	1.45±0.09	1.55±0.20	1.60±0.18
3	1.77±0.15	1.91±0.20	2.11±0.23
4	2.16±0.14	2.21±0.20	2.12±0.25
5	1.90±0.17	2.00±0.10	2.28±0.28
6	2.74±0.21	2.54±0.25	2.53±0.27
7	2.11±0.19	2.33±0.15	2.09±0.29
8	1.97±0.18	1.96±0.14	2.27±0.37
9	2.38±0.17	2.40±0.10	2.50±0.33
10	2.68±0.17	2.67±0.08	
13	2.52±0.12		2.69±0.47
14	2.52±0.12	2.56±0.15	

[a]Reference 11.
[b]Values obtained from analyses of reactions (1) assuming LTS and explicit competition with reactions (3).
[c]Average bond energies obtained from analyses of reactions (8) assuming LTS and STS models.

C. Thermochemistry

1. Fe_nD^+

Bond energies for Fe_nD^+ have previously been measured by threshold analyses of the endothermic reactions of Fe_n^+ clusters with D_2 and CD_4.[11,43] In the present study, this thermochemistry can be obtained from analyses of the cross sections for reactions (1) and (8). Needed thermodynamic information includes $D_0(ND_2-D) = 4.81\pm0.01$ eV.[46] For reactions (1), we analyzed the Fe_nD^+ cross sections using a loose transition state (LTS) coupled with explicit consideration of the competition with the low energy dehydrogenation channel, reaction (3), assumed to have a tight transition state (TTS). Bond energies obtained from this procedure are listed in Table I and shown as open circles in Fig. 6s in Ref. 42. These values are in good agreement with the previous data,[11] having a mean absolute deviation (MAD)=0.09 ±0.08 eV for $n=2-10$, 14. It is worth stressing that the competition threshold analysis has no additional optimization parameters (other than the threshold energies for each channel) to adjust compared to the normal threshold analysis that includes lifetime effects.[47] The competition between channels is determined by the ratio of the unimolecular rate constants for each process, as calculated using RRKM theory. Thresholds for both reactions (1) and (3) are simultaneously obtained in this procedure.

Fe_n^+-D bond energies obtained from analyses of the secondary reactions (8) are listed in Table I (see also Fig. 6s in Ref. 42). As discussed above, the data for reactions (8) were analyzed assuming both a LTS and a standard transition state (STS).[42] The average bond energies obtained using the two

TABLE II. $Fe_n^+-ND_3$ bond energies (eV) obtained from analyses of reactions (6) and (12).

n	$Fe_n^+-ND_3$ (6)[a]	$Fe_n^+-ND_3$ (12)[a]
1	2.16±0.29	
2	1.38±0.13	1.88±0.32
3	>2.11±0.20	2.00±0.36
4	0.99±0.24	1.68±0.57
5		2.38±0.59
6		1.51±0.53
7		
8	1.73±0.34	
9	1.83±0.33	

[a]Average value obtained assuming a LTS and a STS.

models are in good agreement with the previously published values (MAD=0.18±0.12 eV) and well within the larger uncertainties associated with these high energy products. (Values using the LTS agree better with our previous data, MAD=0.19±0.10 eV, than values where the STS assumption was used, MAD=0.35±0.22 eV.) Hence, our assumption that energy is efficiently retained by the primary product (Fe_nD^+), which is the EM for this process, appears to be reasonable, even for the smaller clusters.

2. $Fe_nND_3^+$

Bond energies for $Fe_n^+-ND_3$ can be obtained from analyses of the thresholds for reactions (6) and (12) using Eqs. (20) and (22). For reactions (6), the precursors are the $Fe_nND_3^+$ products, whereas for reactions (12) they are the $Fe_{n-1}ND_3^+$ products, as discussed above. Both reactions involve Fe atom loss and therefore the cross sections are analyzed for thresholds using both LTS and STS models. Bond energies are calculated from the average of LTS and STS thresholds obtained from both reactions (6) and (12), Table II. Uncertainties in the latter values are particularly large because of the combined uncertainties of the $D(Fe_{n+1}^+-Fe)$ and $D(Fe_n^+-Fe)$ values, Eq. (22).

The binding energy of ammonia to the iron monomer cation obtained from collision-induced dissociation (CID) studies of $FeNH_3^+$, $D_0(Fe^+-NH_3)=1.90\pm0.12$ eV,[30] is within the uncertainties of the value that we obtain from reaction (6) for the dimer, 2.16±0.29 eV. Values for $D_0(Fe_2^+-ND_3)$ obtained from reactions (6) for the trimer and Eq. (12) for the tetramer are not in good agreement with one another. Indeed the bond energy obtained from analysis of reaction (12) with the tetramer cation yields a bond energy that exceeds $D_0(Fe_2^+-Fe)=1.67\pm0.12$ eV, meaning that reaction (6) should be exothermic for the trimer cation. This suggests that formation of $Fe_2ND_3^+$ in reaction (6) is not observed until slightly higher energies because the $Fe_3ND_3^+$ adduct has a sufficiently long lifetime to reach the detector before dissociation, consistent with the relative magnitudes and complementary energy dependences of the cross sections for these two product ions, Fig. 2. However, an RRKM calculation of the lifetime of $Fe_3ND_3^+$ adduct at thermal energies suggests it is only 10^{-8} s, as might be expected for such a small molecule and much shorter than the experimental time available, 10^{-4} s. This calculation assumes that the rate limiting transition state is loose, which may mean that the long-lived $Fe_3ND_3^+$ species observed here has a $DFe_3ND_2^+$ structure in which ammonia elimination requires passing through a TTS.

The bond energy obtained for $Fe_3^+-ND_3$ from reaction (12), 2.00±0.36 eV, is somewhat low but still within the uncertainty of the lower limit established by the observation of an exothermic reaction (6) for Fe_4^+, where $D(Fe_3^+-Fe)=2.11\pm0.20$ eV. As for $Fe_2ND_3^+$, the values obtained from reactions (6) and (12) are not in particularly good agreement with one another for $n=4$, although they do lie within combined uncertainties of one another. As suggested above for the trimer, it seems possible that the apparent threshold for reaction (6) in the Fe_5^+ reaction is delayed because the $Fe_5ND_3^+$ adduct lifetime is longer than the available flight time at the lowest energies. Here, and for all larger clusters, RRKM calculations indicate that the $Fe_nND_3^+$ adducts have lifetimes that exceed the flight time of the ions, even assuming a loose transition state for loss of intact ammonia. Similar considerations for larger clusters would make the values obtained for reaction (6) lower limits. Overall, we find that the binding energies of ND_3 to various sized clusters are all about 2 eV, with fluctuations that presumably reflect whether there is a good acceptor orbital on the clusters for the ammonia lone pair of electrons. Values for the largest clusters derived here ($n=8$ and 9) are about 1.8 eV (Table II) and can be compared to those measured on large neutral iron clusters ($n=19,23,26,29,32,34$) by Parks and Riley.[48] They found that the first ammonia binds to each of these clusters with an energy of 0.88±0.02 eV. Presumably, the charge on the cationic clusters studied here influences this thermochemistry appreciably for a bond that is largely electrostatic. However, other factors may also be operative as larger bond energies (0.8–2.4 eV) have been measured for ammonia bound to a commercial iron catalyst, values that span a similar range to the bond energies measured here.[49]

3. $Fe_nND_2^+$

Iron cluster amidogen (ND_2) cations are observed in reactions (2) for Fe_n^+ ($n=1,4-8$) and in reactions (9) for Fe_n^+ (2–5). If we assume that the cluster amidogen cation products are formed along with FeD in reaction (9a), Eq. (21) can be used to convert these thresholds to bond energies for $Fe_n^+-ND_2$, whereas Eqs. (19) and (20) are needed for processes (2) and (9b), respectively. The results are listed in Table III. The average value for Fe^+-ND_2 obtained from reaction (9a) using LTS and STS models, 2.90±0.15 eV, agrees well with a bond energy obtained from studies of the reaction of Fe^+ with ammonia, $D(Fe^+-NH_2)=3.02\pm0.15$ eV.[29] The value also agrees with results from Buckner and Freiser who used reaction chemistry to bracket this bond energy between 2.5±0.1 and 3.1±0.3 eV.[50] Clearly, $FeND_2^+$ is formed in process (9a) along with FeD as a neutral product for reaction of the dimer, because if reaction (9b) is the assumed pathway, the bond energy obtained would be larger by 1.5 eV, much larger than the literature values. This pathway also seems certain for the trimer reaction, because

TABLE III. $Fe_n^+-ND_2$ bond energies (eV) obtained from analyses of reactions (2) and (9).

n	$Fe_n^+-ND_2$ (2, LTS)	$Fe_n^+-ND_2$ (9)[a]
1	3.02±0.15[b]	2.90±0.15[c]
2		2.29±0.16[c]
3		2.70±0.21[d]
4	2.94±0.15	2.86±0.24[d]
5	2.66±0.10	
6	3.31±0.10	
7	3.22±0.12	
8	3.21±0.20	

[a]Average value obtained assuming a LTS and a STS.
[b]From state-specific reaction studies of Fe^+ (^6D,^4F), Ref. 29.
[c]From reaction (9a).
[d]From reaction (9b).

TABLE IV. Fe_n^+-N bond energies (eV) obtained from analyses of reactions (4) and (11).

n	Fe_n^+-N (4, LTS)[a]	Fe_n^+-N (4, TTS)[b]	Fe_n^+-N (11, STS)[c]	Fe_n^+-N (11, TTS)[d]
1				
2	4.86±0.20	4.86±0.20	5.03±0.45	5.03±0.45
3	4.33±0.10	4.36±0.10	4.72±0.15	4.87±0.15
4	4.72±0.09	4.73±0.09	5.29±0.17	5.19±0.17
5	4.47±0.20	4.46±0.20	4.67±0.23	4.47±0.23
6	4.07±0.10	4.36±0.10	4.40±0.27	4.23±0.27
7	3.64±0.26	4.06±0.26	3.97±0.33	3.99±0.33
8	3.97±0.20	4.36±0.20	4.32±0.31	4.26±0.31
9	3.74±0.25	4.22±0.25	4.15±0.29	4.18±0.29
10	3.60±0.25	4.16±0.25		
14	3.79±0.25	4.21±0.25		

[a]Fe_nND^+ precursor, loose transition state.
[b]$Fe_nND_2^+$ precursor, tight transition state.
[c]Average value obtained assuming a LTS ($Fe_{n-1}ND^+$ precursor) and a STS (Fe_nN^+ precursor).
[d]$Fe_{n-1}ND_2^+$ precursor, tight transition state.

the alternate assumption of concomitant formation of Fe+D in reaction (9b) yields a bond energy of 3.78±0.15 eV for $Fe_2^+-ND_2$, much too large to be reasonable.

Oddly, the mechanism for reaction (9) seems to switch from Eq. (9a) for the dimer and trimer to Eq. (9b) for the tetramer and pentamer. In the latter case, this is shown by good agreement between the bond energy obtained for $Fe_4^+-ND_2$ from reaction (2) assuming a LTS and that obtained from reaction (9b) for the pentamer, Table III. Hence, we believe that $Fe_3ND_2^+$ is produced in reaction (9b) for the tetramer system as well because if reaction (9a) were operative, the bond energy derived would be 1.5 eV smaller and inconsistent with the trends discussed below. This conclusion is further supported by the sum of the $Fe_3ND_2^+$ and $Fe_4ND_2^+$ cross sections in the tetramer system, which shows a smooth energy dependent behavior. Bond energies for $n=5-8$ are derived only from reactions (2) assuming a LTS as reactions (9) were not observed for the larger clusters (although this is probably because the cross sections are small, not because the reactions do not occur at all). Trends in the thermochemistry are discussed below.

4. Fe_nN^+

Bond energies for Fe_n^+-N can be obtained from analyses of reactions (4) and (11). For larger cluster sizes, the thresholds for these reactions are less reliable than for other reactions because the cross sections needed to be corrected for mass overlap with the Fe_nND^+ product, which is much more intense in the threshold region of Fe_nN^+. The required thermochemistry is $D(ND_3-L)=D(ND-D_2)+D(N-D)=7.86\pm0.01$ eV.[46] For reactions (4), the precursors are either the primary Fe_nND^+ or $Fe_nND_2^+$ products, whereas for reactions (11), we consider Fe_nN^+, $Fe_{n-1}ND^+$, and $Fe_{n-1}ND_2^+$ as possible precursors. Therefore, cross sections are analyzed for thresholds using a TTS model associated with D_2 loss for reactions (4) and (11), a LTS model associated with D atom loss for both reactions (4) and (11), and a STS model for the Fe atom loss in reactions (11). The results are given in Tables S2–S11 with the derived bond energies summarized in Table IV and also shown in Fig. 7s of the supplementary material.[42] Bond energies obtained from analyses of reactions (11) are not particularly sensitive to the TS assumptions made. These values are in reasonable agreement with bond energies obtained from reactions (4), and show similar variations with cluster size. There is overall better agreement with BDEs from reaction (11) when a TTS is assumed for reaction (4), MAD of 0.18±0.19 eV for $n=2-9$, compared to when a LTS is assumed, MAD of 0.33±0.15 eV. Note that the bond energies from reactions (11) are generally higher than those from reactions (4), whereas if the multiple neutral products carried away excessive amounts of energy, the thresholds would be high and the resultant bond energies low. It might also be noted that the bond energies in Table IV assume that the neutral products in reactions (11) are Fe+D+D_2, whereas FeD+D_2 products are also possible. If this were happening, the Fe_n^+-N bond energies would be 1.49±0.04 eV[44,45] higher in energy and no longer agree with values from reactions (4). Further, as noted above, evidence for FeD loss is observed for the dimer and trimer reactions but not for larger clusters.

Of these various bond energies, the average of those obtained from analyses of reactions (11) and reactions (4) with a TTS are considered our best values because they are systematically larger, suggesting that the analysis successfully avoids the possibility of competition with other channels. Note also that this agreement tends to suggest that the Fe_nN^+ products are formed by D_2 elimination from $Fe_nND_2^+$. The maximum Fe_n^+-N bond energy is recorded for the tetramer. For larger clusters, the binding energies to N reach a rough plateau near 4.2±0.1 eV ($n=6-10,14$).

5. Fe_nND^+

Bond energies for Fe_n^+-ND can be obtained from analyses of the thresholds for reactions (3), (10), and (13) using Eqs. (19), (20), and (22), respectively, and $D_0(ND-D_2)=4.35\pm0.01$ eV.[46] As discussed above, the data for reactions (3) were analyzed assuming a TTS. Competition with reaction (1) is also explicitly considered but this does not alter the thresholds obtained for reactions (3). The resultant bond energies are listed in Table V. Reactions (10) and (13)

TABLE V. Fe_n^+–ND bond energies (eV) obtained from analyses of reactions (3), (10), and (13).

n	Fe_n^+–ND (3, TTS)	Fe_n^+–ND (10)[a]	Fe_n^+–ND (13)[a]
1			
2	2.43±0.23	3.42±0.16	3.80±0.26
3	>4.35 (3.40±0.20)[b]	4.72±0.21	4.43±0.35
4	>4.35 (4.00±0.10)[b]	5.15±0.23	5.41±0.40
5	>4.35 (3.57±0.15)[b]	4.68±0.26	4.45±0.53
6	3.24±0.07	4.22±0.29	
7	3.11±0.10	4.12±0.28	
8	3.31±0.10	4.30±0.36	
9	3.61±0.10	4.38±0.34	
10	3.55±0.08	Est 4.50±0.13	
13		4.82±0.51	
14	3.30±0.15	Est 4.25±0.18	

[a]Average bond energy obtained from LTS and STS models.
[b]Value obtained from analysis of the endothermic feature in the cross section for reaction (3).

correspond to loss of one or two Fe atoms from the Fe_nND^+ primary product and are therefore analyzed using both LTS and STS models.

The values obtained from reactions (10) and (13) are in reasonable agreement, with a MAD of 0.29±0.07 eV and an average signed deviation of 0.03±0.33 eV, well within the experimental uncertainties, Fig. 7. In addition, it can be seen that the values for $n=3-5$ exceed D(ND–D_2), consistent with the observation of an exothermic reaction (3) for these three clusters. Other sized clusters have Fe_n^+–ND bond energies lower than this value, with the possible exception of the largest clusters studied here ($n\geqslant 9$), although these could have bond energies lower than D(ND–D_2) as well. In contrast to this good agreement, the bond energies obtained from reaction (3) are much lower than those from reactions (10) and (13). For the five systems where multiple values are available ($n=2$,6–9), the thresholds of reactions (3) lead to bond energies that average 0.95±0.10 eV lower than those

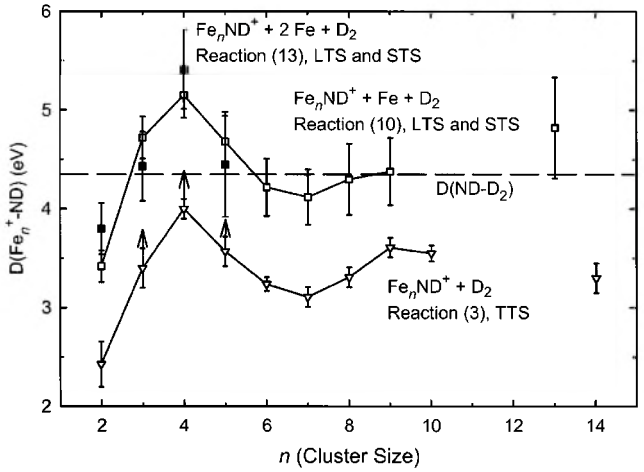

FIG. 7. Fe_n^+–ND bond energies (Table V) obtained from analyses of reactions (3) (open triangles), (10) (open squares), and (13) (solid squares). The dehydrogenation energy of ammonia, 4.35 eV, is shown by the horizontal dashed line. Values from reactions (3) for $n=3-5$ are evaluated from the endothermic feature in the cross section (see text) and are therefore lower limits to the true bond energy, as indicated by the arrows.

from reaction (10). The discrepancy between the results for the primary and secondary (and tertiary) reactions are sensibly attributed to a barrier along the reaction path of about 0.95±0.10 eV in excess of the endothermicity for the dehydrogenation reactions (3) with Fe_n^+, except for $n=3-5$. This indicates that the use of the TTS model for reaction (3) is appropriate. Use of an STS or LTS model would increase the thresholds, thereby lowering the derived bond energies further and increasing the discrepancy with the bond energies derived from analysis of reactions (10) and (13). Such a barrier is consistent with our previous demonstration that there is also a barrier (0.7±0.3 eV for $n>6$) in the analogous dehydrogenation reaction of methane, $Fe_n^+ + CD_4 \rightarrow Fe_nCD_2^+ + D_2$.[43] Only Fe_3^+ and Fe_4^+ did not exhibit signs of a barrier to this reaction with methane. In the present system, the barrier maintains a consistent magnitude for all clusters where data are available, such that we also use the 0.95±0.10 eV barrier height to estimate values for D(Fe_n^+–ND) for $n=10$ and 14 from the threshold values for reactions (3).

As noted in the results, the cross sections for formation of Fe_nND^+ ($n=3-5$) exhibit two features, one corresponding to an exothermic and barrierless process and the other exhibiting a barrier. Analysis of the endothermic portions of these reactions provides thresholds that can be converted to the bond energies listed in Table V and shown with arrows in Fig. 7. It can be seen that these values again parallel those obtained from reactions (10) and lie an average of 1.19±0.11 eV below those values. This is comparable to the "barrier" height derived above, suggesting that the primary pathway for dehydrogenation has a barrier in all systems, but that when the reaction is exothermic, an alternate pathway can be found, as discussed further below. For cases in which the exothermicity is small ($n=3$ and 5), this alternate pathway is inefficient, but for $n=4$, where the reaction is exothermic by 0.8±0.2 eV, the process occurs much more efficiently. Results are ambiguous for the larger clusters ($n\geqslant 10$) because of the large uncertainties in the bond energies and because the energy necessary to drive this process may dissipate through the larger clusters, thereby reducing the efficiency of the alternate pathway.

The present results do not provide a value for D(Fe^+–ND). This has been measured using photodissociation by Buckner *et al.* as 2.65±0.22 eV,[51] but an analysis of the periodic trends in first row metal ligand bond energies suggests that this value is too low.[44] Using ion-molecule reactions, Brönstrup *et al.* determined a value of 2.99±0.09 eV,[52] which agrees nicely with $D_0(Fe^+–ND)=3.04\pm0.15$ eV determined in our complementary study of the state-specific reactivity of Fe^+ with ND_3 determined from a collision-induced dissociation experiment.[29]

6. $DFeND_2$

In all of the cluster systems, we observe evidence for reaction (7b) in which $FeND_3$ is produced as the neutral product. The difference between the threshold for this reaction and that for simple CID, taken from our previous work,[25] is the bond energy for Fe–ND_3. Data for the reactions with Fe_4^+ and Fe_5^+ are the most precise and give an

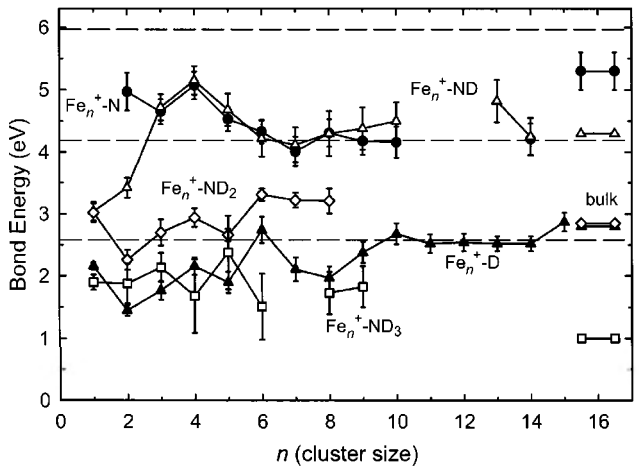

FIG. 8. Comparison of bond energies for Fe_n^+-D (solid triangles, taken from Ref. 11), $Fe_n^+-ND_3$ (open squares, Ref. 30, and this work, Table II), $Fe_n^+-ND_2$ (open diamonds, this work, Table III, see text), Fe_n^+-ND (open triangles, Ref. 29 and this work, Table V), and Fe_n^+-N (closed circles, this work, Table IV). Bulk phase values for iron surfaces binding D (Refs. 59–61) and ND_3 (Ref. 49) and estimates for N (Refs. 60 and 61), ND and ND_2 (Ref.18) are also shown to the right. Horizontal dashed lines provide estimates for single, double, and triple bonds to iron clusters based on information in Ref. 43.

average value of 1.16 ± 0.27 eV. Contributions to this process are evident for larger clusters but not as distinct, making threshold interpretation less accurate.

The structure of the $FeND_3$ molecule lost in these processes could involve an intact ammonia ligand or potentially correspond to an inserted D–Fe–ND_2 complex. To investigate this, theoretical calculations were performed for both geometries. All quantum chemistry calculations here are computed with the B3LYP hybrid density functional method,[53–55] and performed with the GAUSSIAN 98 suite of programs.[56] Geometry optimizations and vibrational frequency calculations used a 6-31+G* basis set and single point calculations used a 6-311++G($3df$,$3p$) basis. These calculations indicate that $HFeNH_2$ is the more stable geometry by 0.544 eV. This species has a $^5A_1$ ground state with C_{2v} symmetry and r(Fe–H)=1.639 Å, r(Fe–N)=1.861 Å, r(N–H)=1.017 Å, ∠HFeN=180.0°, ∠FeNH=125.9°, and ∠HNH=108.2°. The $FeNH_3$ connectivity has a $^5A_1$ ground state with C_{3V} symmetry and r(Fe–N)=2.166 Å, r(N–H)=1.024 Å, ∠FeNH=111.1°, and ∠HNH=107.8°. Compared to the Fe(^{5}D,$4s^2 3d^6$)+NH_3($^1A_1$) ground state asymptote, these species are bound by 0.989 and 0.445 eV, respectively, including zero point energies (adjusted by a factor of 0.9804)[57] and a correction of 0.050 eV for the properly weighted mean energy of all spin-orbit levels in the Fe(^{5}D) ground state term. Our experimental value of 1.16 ± 0.27 eV agrees nicely with the former value but not the latter, strongly suggesting that we are observing the $DFeND_2$ inserted species as the neutral $FeND_3$ product.

V. DISCUSSION

A. Bond energies

Our recommended set of bond energies between iron cluster cations and the D and ND_x (x=0–3) ligands are shown in Fig. 8. The Fe_n^+-D values are taken from our previous work on reactions of $Fe_n^+ + D_2$.[11] Results from the present study substantiate these values but analyses of the D_2 reaction cross sections are less problematic than those for the ND_3 reaction system because there is no competition with other products in the D_2 system. $Fe_n^+-ND_3$ bond energies are those listed in Table II obtained from analyses of the secondary reactions where available and the literature for n=1.[30] $Fe_n^+-ND_2$ bond energies are those listed in Table III and are weighted averages in the cases of n=1 and 4. The Fe_n^+-N values are average values of those derived from analyses of reactions (11) and reactions (4) with a TTS, Table IV. The best Fe_n^+-ND values are obtained from reactions (10) using the average thresholds obtained from LTS and STS assumptions, Table V, except for the $FeND^+$ value of 3.04 ± 0.15 eV, which is taken from a more detailed state specific study of the $Fe^+ + ND_3$ system.[29]

In general, the trends in these cluster-ligand bond energies can be understood by considering the maximum number of bonds that the ligands can make with the cluster. D(^{2}S) can make only a single covalent bond with the cluster, and the trends observed with cluster size in the Fe_n^+-D BDEs reflect the variations in the electronic structure of the cluster, as discussed in detail before.[11] Note that the cluster cation bond energies to ND_2 ($^2B_1$), which can also make a single covalent bond to the cluster, parallel the Fe_n^+-D bond energy curve. This reflects the common electronic character of the variations observed and helps verify their accuracy. On average, the $Fe_n^+-ND_2$ bond energies are 0.78 ± 0.13 eV higher in energy than the Fe_n^+-D values for the cluster sizes n=1–6. The enhancement is somewhat larger for n=7 and 8, 1.18 ± 0.09 eV. These enhanced bond energies must be the result of a dative bond formed by donating the lone pair of electrons on nitrogen to the cluster. In an analysis of the periodic trends in bond energies for first row transition metal ions, M^+-NH_2 vs $M^+-CH_3 \approx M^+-H$,[44] it was found that early metals (Sc–V) with empty acceptor orbitals had amide bonds that were about 1.2 ± 0.2 eV stronger than the methyl bonds, whereas late metals (Mn–Ni) with singly occupied acceptor orbitals had an average enhancement of only 0.5 ± 0.2 eV (with iron at the top of this range). The 0.78 ± 0.13 eV enhancement observed here for the iron cluster cations indicates that clusters can accept electron density more efficiently than the late atomic metal ions, although not with the facility of the early metal ions. This suggests that the clusters can move electron density around to enhance the bonding but perhaps not to the point of completely emptying the acceptor orbital involved. For n=7 and 8, we hypothesize that an asymptotic value for $Fe_n^+-ND_2$ BDEs of large clusters has been reached, whereas the weaker Fe_n^+-D BDEs do not reach their large cluster limit until about n=10, Fig. 8. This suggestion is rationalized further below.

It can be seen that the Fe_n^+-D bond energies and the $Fe_n^+-ND_3$ bond energies are more or less comparable for n=1–3, whereas the pattern inverts for n=4–6 although the average bond energies are in the same range. Presumably this reflects the differences in the abilities of the cluster cations to form a covalent bond with D (thereby requiring a singly occupied orbital) versus forming a dative bond by accepting

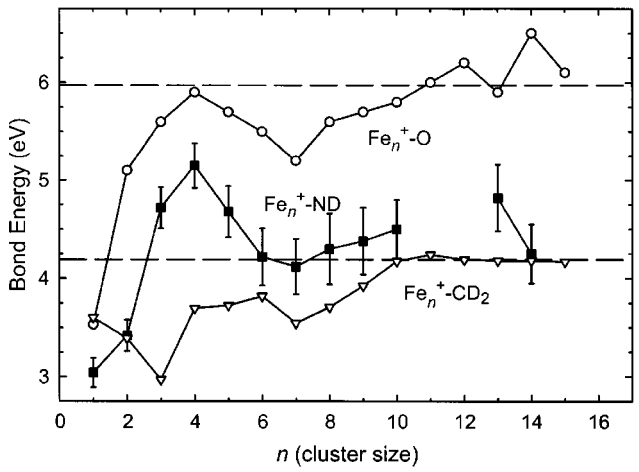

FIG. 9. Comparison of bond energies to iron cluster cations of the isoelectronic ligands, ND (solid squares, Ref. 29 and this work, Table V), CD_2 (open triangles, Ref. 43), and O (open circles, Ref. 10). Horizontal dashed lines provide estimates for double and triple bonds to iron clusters based on information in Ref. 43.

a pair of electrons into a largely empty orbital. In our work on the reactions of $Fe_n^+ + D_2$,[11] our analysis of the $Fe_n^+ - D$ bond energies focused on the molecular orbitals formed from the atomic $4s$ orbitals, and these same orbitals should be pertinent for bonding to ND_3. For these MOs, the variations in $Fe_n^+ - D$ bond energies suggested ground state electronic configurations of σ_g^2 for Fe_2^+, $1a_1^2 2a_1^2 1b_2^0$ for Fe_3^+ (bent), $a_1^2 e^3$ for Fe_4^+ (tetrahedral), $1a_1^2 1b_1^2 1b_2^2 2a_1^0$ for Fe_5^+ (trigonal bipyramid), and $a_{1g}^2 t_{1u}^5$ for Fe_6^+ (octahedral). The atomic case of $FeND_3^+$ has been discussed previously[30] and calculations indicate that it corresponds to a sextet state in which ammonia donates its lone pair of electrons into the singly occupied s orbital of the $Fe^+(^6D,4s^1 3d^6)$ ground state. Apparently when there is a low-lying empty valence orbital (such as for $n=3$ and 5), the bond to ammonia is stronger than when the only empty orbitals are antibonding ($n=2$, 4, and 6).

The ND fragment can form two covalent bonds, much like the isoelectronic CD_2 and O atom fragments. A comparison of $Fe_n^+ - ND$ and $Fe_n^+ - CD_2$ bond energies,[43] Fig. 9, shows that they parallel one another closely for $n \geqslant 6$, where the bonds to ND are stronger by an average of 0.5 ± 0.1 eV. This enhancement can again be attributed to the dative interaction of the lone pair of electrons on nitrogen donating to the iron cluster. The enhancement is slightly weaker than that for ND_2, suggesting that there are either overlap differences resulting from different amounts of p character in the lone pairs of ND_2 vs ND or that the electronic structure of the iron clusters alters somewhat because of the formation of one vs two covalent bonds with ND_2 vs ND, respectively. A similar comparison to the $Fe_n^+ - O$ bond energies,[10] isoelectronic with both $Fe_n^+ - ND$ and $Fe_n^+ - CD_2$, again show parallel trends for $n \geqslant 6$, Fig. 9. Here the bonds to O are stronger by an average of 1.3 ± 0.1 eV than bonds to ND. For the smaller clusters, the $Fe_n^+ - ND$ and $Fe_n^+ - CD_2$ bond energies differ appreciably. For the monomer, the $Fe^+ - ND$ bond is somewhat weaker than $Fe^+ - CD_2$ and $Fe^+ - O$, which are very similar, suggesting little dative bond enhancement. For $n=2$, the $Fe_2^+ - ND$ and $Fe_2^+ - CD_2$ bond energies are now nearly equivalent, whereas the $Fe_2^+ - O$ bond energy is much stronger. Clearly, the details of the electronic structure for the monomeric and dimeric species are controlling features in these various bonds. In contrast, the $Fe_n^+ - ND$ bond energies for $n=3-5$ are much stronger than those for $Fe_n^+ - CD_2$, by 1.8, 1.5, and 1.0 eV, respectively. This is largely because the $Fe_n^+ - CD_2$ bond energies are relatively weak, e.g., $D(Fe_3^+ - CD_2) = 2.97 \pm 0.09$ eV. This is also illustrated by the observation that these three $Fe_n^+ - ND$ bond energies more closely parallel the analogous $Fe_n^+ - O$ bond energies, Fig. 9, which are stronger by an average of 0.9 ± 0.1 eV. Thus, the $Fe_n^+ - ND$ bond energies for these small clusters are more comparable to those of larger clusters than the $Fe_n^+ - CD_2$ analogues, similar to the observations for the $Fe_n^+ - O$ analogues. Nevertheless, it is interesting that the $Fe_n^+ - ND$ bond energy for $n=4$ is the largest measured here, suggesting that this cluster does have some unique thermodynamic properties with regard to binding this particular ligand. Another way of thinking about the differences in the binding of CD_2, ND, and O focuses on the structure. Thus, CD_2 is likely to bind in bridging position between two metal atoms, and this geometry is also available to the ND and O species. However, these latter two species may also bind in three-fold sites by using one of their lone pairs of electrons. Indeed, this is the geometry obtained by Fossan and Uggerud for Fe_4NH^+ in their calculations.[17] It is possible that the differences in the ND bond energies measured here as a function of size are related to variations in the ground state structure of the various Fe_nND^+ species.

Bond energies for $Fe_n^+ - N$ are very similar to those for $Fe_n^+ - ND$ with the exception of the values for $n=2$, lying within 0.2 eV of one another for $n \geqslant 3$, Fig. 8. Although the trend with cluster size seems reasonable, the $Fe_n^+ - N$ bond energies measured here seem anomalously weak. This is because $N(^4S)$ is capable of forming three covalent bonds and we have previously shown that iron clusters can form triple bonds with CD, C, and O that have bond energies of about 6.0 eV for the larger iron cluster cations.[9,10,43] A direct comparison of the $Fe_n^+ - N$ and $Fe_n^+ - CD$ bond energies finds that they are similar for $n=3$ and 4, the latter are stronger by about 0.85 ± 0.1 eV for $n=5-10$, and the difference is about 2 eV for $n=14$. It is unclear why the nitrogen atom does not form bonds more comparable to CD with the larger iron cluster cations, although differences in hybridization of the orbitals on CD vs N could be influential. One possibility is simply that the thresholds measured here for these high energy products with the larger clusters are inaccurate because of the difficulties noted above in measuring the Fe_nN^+ and $Fe_{n-1}N^+$ cross sections in their threshold region. Alternatively, it is possible that if the pathways for reactions (4) and (11) are primarily by dehydrogenation of $Fe_nND_2^+$ and $Fe_{n-1}ND_2^+$, then there could be barriers to both reactions or the TTS involved could make these processes susceptible to particularly large competitive shifts, which were not explicitly considered here.

Overall, our present results are qualitatively consistent with iron clusters cations forming a single covalent bond

with D, a single dative bond with ND_3, a single+dative bond with ND_2, and a double+dative bond with ND. The bonding character of the N atom ligand is generally close to a double bond, in contrast to simple expectations.

B. Bond energies compared to bulk phase values

One area where cluster studies may provide insight into condensed phase chemistry lies in the determination of thermochemistry for molecular fragments bound to surfaces. We have previously noted that bond energies of oxygen atoms to iron cluster cations larger than 2 atoms are relatively constant at about 5.8 ± 0.3 eV,[10] and match bulk phase heats of adsorption of oxygen to iron surfaces, 4–5.5 eV.[58] Likewise, Fe_n^+-D bond energies reach a relatively constant value (Fig. 8) of about 2.61 ± 0.14 eV for $n\geqslant10$. This is close to the bulk phase value for hydrogen binding to bulk iron surfaces, about 2.8 eV for measurements on Fe(100), Fe(110), and Fe(111) surfaces.[59–61]

For nitrogen based species, the binding of N atoms to Fe(100), Fe(110), and Fe(111) surfaces have been measured as about 6.0 ± 0.1 eV by using temperature-programmed desorption of N_2 on these surfaces.[60–62] However, dissociative chemisorption of N_2 on iron surfaces is estimated to have an activation barrier greater than about 0.4 eV, such that these values are upper limits to the true atomic bond enthalpies by at least this much. Alternatively, the adsorption bond energies to surfaces can be estimated from bulk compounds and in the case of Fe_4N, this leads to an estimate for the atomic adsorption energy of 5.0 eV.[61] These estimated values for binding of N atoms to iron surfaces, 5.0–5.6 eV are comparable to the largest Fe_n^+-N bond energies measured here ($n=2-4$, Table IV, Fig. 8), but substantially larger than the average values for larger clusters, 4.2 ± 0.1 eV for $n\geqslant6$. As noted above, these Fe_n^+-N bond energies appear somewhat small compared to previous measurements on Fe_n^+-CD species,[43] for reasons that are unclear. One possible effect is suggested by calculations of Nørskov and co-workers, who found that nitrogen atoms bind most strongly to iron surfaces in four-fold sites, e.g., on Fe(100), whereas binding to the (111) and (110) surfaces is weaker by 0.7 eV.[63] As small clusters will generally have three-fold but no four-fold sites, this could explain the weaker bonds observed here.

In contrast to the atomic H, O, and N systems, there is virtually no experimental information on the thermochemistry of NH and NH_2 bound to metal surfaces, although such information has been estimated.[18] As discussed above, the successful comparison of surface adsorption energies for H and O atoms to the bond energies for larger cluster ions suggests that such cluster values can be used to estimate surface energies for molecular fragments that are largely inaccessible to experimental measurement. This was argued in our analogous work for the organic fragments, C, CD, and CD_2,[43] and should be suitable for the ND and ND_2 fragments measured here, especially as the patterns discussed above behave sensibly compared with the previously measured bonds to CD_2 and D. Thus, the present work estimates that the binding of ND_2 to iron surfaces should be about 3.25 ± 0.10 eV on the basis of the values for the three largest clusters studied ($n=6-8$, Table III). Alternatively, the enhancement resulting from the dative bond, an average of 0.78 ± 0.13 eV, can be added to the large cluster ($n\geqslant10$) average of $D(Fe_n^+-D)=2.61\pm0.14$ eV to yield an estimate of about 3.4 ± 0.2 eV for $D(Fe_n^+-ND_2)$. These estimates are in reasonable agreement with one another, suggesting that the $n=6-8$ clusters have nearly approached the bulk phase limit. This can explain why the bond enhancement for ND_2 versus D for $n=7$ and 8 is larger than for smaller clusters, Fig. 8, as the Fe_nD^+ clusters do not reach the bulk phase limit until somewhat larger clusters, $n\geqslant10$. On iron surfaces, the bulk phase adsorption energy for NH_2 has been estimated as equivalent to that for H, or about 2.8 eV.[18] The present data illustrate that such an estimate is inaccurate and misses the important dative component of the binding of NH_2 to metals.

For the ND fragment, bond energies for the largest clusters available suggest a value of 4.5 ± 0.3 eV. A comparable value of 4.7 ± 0.4 eV is obtained by taking the average $Fe_n^+-CD_2$ bond energies for large clusters, 4.2 ± 0.4 eV, and adding the average enhancement of 0.5 ± 0.1 eV observed for Fe_n^+-ND bond energies. These bond energies can be favorably compared to previous estimates for NH_{ad} of about 4.3 eV.[18] Again this estimate fails to incorporate the dative enhancement of the bonding of NH to metals.

C. Reaction mechanism

The mechanism for reactions of iron cluster cations with ammonia should parallel those for any sigma bond activation process. Presumably, a physisorbed adduct, $Fe_n^+(ND_3)$, is formed initially and should be fairly stable because of the attractive long-range ion dipole interaction. Bond energies for such species, Table II, vary appreciably but all lie in the range of about 1.4–2.4 eV. For all clusters but the dimer, the adduct is observed at low energies. For clusters larger than five atoms, it is the only product observed at thermal energies. The adducts can decompose back to reactants or they can lose an Fe atom, the exchange reaction (6), which is competitive because the $Fe_n^+-ND_3$ bond energies are comparable to the Fe_{n-1}^+-Fe bond energies.

At some point, sufficient energy is available that the clusters activate an ND bond, thereby forming $D-Fe_n^+-ND_2$ intermediates. These species can decompose at higher energies by simple bond cleavage to form $Fe_nD^+ + ND_2$ or $Fe_nND_2^+ + D$. The former channel is greatly favored over the latter because of conservation of angular momentum effects.[31–33] Simply, the reduced mass of the $Fe_nND_2^+ + D$ product channel is about 2 amu, whereas that for the $Fe_nD^+ + ND_2$ product channel approaches 18 amu, comparable to the reduced mass of the $Fe_n^+ + ND_3$ reactants (about 20 amu). Because orbital angular momentum is largely conserved in these bimolecular reactions, the phase space available to the $Fe_nND_2^+ + D$ product channel is much smaller than that associated with the $Fe_nD^+ + ND_2$ product channel. For reactions of Fe_2^+ and Fe_3^+, we also observe formation of $Fe_{n-1}ND_2^+ + FeD$, reaction (9a), which indicates that the D and ND_2 fragments can be attached at separate sites on the cluster. Presumably this channel is not observed for larger clusters because of competition with more probable reaction

channels. We also observe loss of neutral $FeND_3$, which theoretical calculations indicate has a $DFeND_2$ structure. Thus, the chemisorbed fragments can also attach to the same iron metal center.

The $D–Fe_n^+–ND_2$ intermediates decompose at lower energies by dehydrogenation. This process could involve elimination of D_2 through a rearrangement of the $D–Fe_n^+–ND_2$ intermediate to a four-centered transition state involving an incipient D–D bond (the pathway followed by the monomer),[29,43] or as the clusters get larger, the D and ND_2 fragments can bind to separate sites such that the transition state becomes less strained. Finally, for larger clusters, it is also possible that a $(D)_2Fe_n^+–ND$ species could be generated and reductively eliminate D_2. Because the Fe_nD^+ and Fe_nND^+ products share the common $D–Fe_n^+–ND_2$ intermediate, they compete directly with one another. Thus, once the energy necessary to form the Fe_nD^+ product is exceeded, this product dominates because simple cleavage of the Fe–N bond is kinetically more facile than the more complicated rearrangement needed for dehydrogenation. Thus, the cross sections for the Fe_nND^+ products formed at lower energies begin to decline, Figs. 1–5, indicating that the putative $D–Fe_n^+–ND_2$ common intermediate is being depleted. This competition is also indicated by the fact that accurate Fe_nD^+ bond energies are obtained from the observed thresholds only when competition with dehydrogenation is explicitly considered.

The dehydrogenation process is exothermic for $n=3–5$ but efficient for only $n=4$. For all other clusters, this process exhibits a barrier of about 0.95 eV above the product asymptote. Even for the $n=3–5$ clusters, there is an endothermic feature in the cross sections that corresponds to a barrier of approximately this magnitude. A plausible scenario that emerges from these observations is that there is a crossing between the potential energy surface corresponding to physisorption of ammonia to the iron cluster cation and that corresponding to chemisorption (which can be viewed as evolving from separated D and ND_2 fragments covalently bonding to the cluster). Such an assignment is consistent with conclusions drawn about the activation barriers observed for CD_4 bond activation by Fe_n^+ and for D_2 activation by Cr_n^+ and Fe_n^+.[8,11,43] For most clusters, the surface crossing occurs above the asymptote of the reactants and moves in concert with the overall endothermicity of the reaction, i.e., the asymptote of the products. When the overall reaction is exothermic and the barrier is lower, as it is for $n=3–5$, the reaction continues to proceed over the barrier, leading to the endothermic features in the cross sections, Figs. 2–4; however, there is an alternate pathway that bypasses this barrier. This pathway is inefficient for $n=3$ and 5 (reaction probability of about 0.1%), but occurs with about 5% probability for $n=4$ (12% given more time as in the ICR experiments).[17] This alternate low-energy pathway could conceivably involve coupling between surfaces of different spin, a process that is only efficient when the crossing point is accessed at low kinetic energies. If so, then the higher energy pathway could be assigned to a spin-conserving process. This postulate presumes that such alternate pathways probably exist for other sized clusters but are inefficient because the crossing point is accessed at higher energies than in the $n=3–5$ cluster systems. Another possibility presumes that for larger clusters, it is straightforward to produce a $(D)_2Fe_nND^+$ intermediate in which the three ligands are located remotely on separate metal atoms or different bridging sites. Reductive elimination of D_2 from these intermediates leads to the dehydrogenation reaction observed for most clusters and the endothermic features in the $n=3–5$ cluster cations. For these smaller clusters, the ligands cannot be as remote from one another such that there may be a more concerted process that can lead to dehydrogenation with a lower barrier. Such concerted processes would exist for the larger clusters but be less likely because of the relative stability of the $(D)_2Fe_nND^+$ intermediates.

Some insight into the possibilities discussed above are revealed by recent calculations of the dehydrogenation reaction on Fe_4^+. Fossan and Uggerud[17] performed density functional calculations (B3LYP/LANL2DZ) and found that the lowest energy structure for Fe_4^+ has a spin quantum number of 13/2 and a geometry of a planar rhomboid. Interaction with ammonia proceeds by first binding NH_3 in a deep potential well, then activating first one then a second N–H bond. The latter is the rate-limiting step (although the first activation step is close in energy) and is concerted in that H_2 is formed directly in a four-centered TS, rather than passing through a dihydride $(H)_2Fe_4NH^+$ intermediate. Most interesting is that the Fe_4^+ cluster transforms from the rhomboid to a tetrahedral structure in which the NH is bound to a three-fold site on one face. It is plausible that this structural rearrangement provides the low energy path for dehydrogenation and that the high energy path observed here keeps the original rhomboid structure intact or perhaps involves a dihydride $(H)_2Fe_4NH^+$ intermediate. Alternatively, the calculations also find a parallel reaction surface having a spin quantum number of 11/2, although here the Fe_4^+ starts out nearly tetrahedral and the rate-limiting step has a relatively higher energy. It is feasible that interaction with this surface could provide the high energy pathway to dehydrogenation.

In all cases, the mechanisms gleaned from the present work are consistent with the step-wise activation of ammonia hypothesized for ammonia synthesis on iron surfaces.[18] Clearly on a surface, adsorbed hydrogens are easily moved to remote sites such that dehydrogenation would ordinarily not occur in a concerted step. Thus, the reactivity observed here for larger clusters should parallel the surface chemistry most closely, whereas the chemistry observed for the $n=3–5$ clusters does present a pathway for the dehydrogenation step that appears to be unique to clusters.

VI. CONCLUSION

The kinetic energy dependences of the reactions of size-specific iron cluster cations ($n=2–10,14$) with deuterated ammonia are examined in a guided ion beam tandem mass spectrometer. We report cross sections for about 13 reactions for each cluster system ($Fe_n^+ + ND_3$), most of which exhibit thresholds. Reactions that occur at thermal energies include formation of the adduct, $Fe_nND_3^+$, for all clusters but the dimer; dehydrogenation, reaction (3), for the trimer, tetramer,

and pentamer; and the exchange reaction (6) for the tetramer. For the three systems exhibiting exothermic dehydrogenation, there is also a higher energy feature that appears to match the reactivity observed for other cluster sizes. Dominant reactions at higher collision energies include the dehydrogenation reactions (3) followed by Fe atom loss, reactions (10), and reactions (1) to form Fe_nD^+. Analyses of the energy dependence of primary, secondary, and tertiary routes to the various products provide multiple independent routes to bond energies for each cluster to D, N, ND, and ND_2. The values obtained from these various routes are in reasonable agreement with one another except in the case of ND. The discrepancy is evidence that there are barriers of about 1 eV in excess of the endothermicity of the initial dehydrogenation reaction, except for $n=3-5$. Even in these three cases, endothermic features in the cross sections suggest that a pathway having a comparable barrier is an available reaction pathway. Analysis of the reaction mechanism suggests that this barrier lies in the entrance channel for the initial chemisorption process.

Best estimates for N, ND, ND_2, and ND_3 binding energies to cationic iron clusters are provided from an analysis of these multiple reaction pathways. The relative magnitudes in D, ND, and ND_2 bond energies to the iron cluster cations are consistent with simple bond order considerations and an enhancement of the bond provided by a dative interaction between the lone pair electrons on nitrogen and the cluster. Comparison of these values to limited experimental information for binding of atoms to surfaces suggests that our experimental bond energies for larger clusters should provide reasonable estimates for heats of adsorption to surfaces. As no experimental information is available for molecular species binding to surfaces, the thermochemistry derived here for clusters bound to ND and ND_2 provides some of the first experimental thermodynamic information on such molecular species. These values exceed previous estimates for such thermochemistry[18] because such estimates did not consider the enhancement provided by the dative bonding. Our maximum bond energies obtained for N binding to iron cluster cations are in reasonable agreement with the iron nitrogen binding energy estimated from bulk iron nitrides, although larger clusters have bond energies that appear relatively weak.

ACKNOWLEDGMENTS

This work is supported by the Chemical Sciences, Geosciences, and Biosciences Division, Office of Basic Energy Sciences, Office of Science, U.S. Department of Energy. The authors thank F. Liu for taking data on the Fe_n^+ $(n=3-5)$ $+NH_3$ systems and E. Uggerud for providing results of his work before publication.

[1] G. A. Somorjai, *Chemistry in Two Dimensions: Surfaces* (Cornell University, Ithaca, 1981).
[2] P. B. Armentrout, D. A. Hales, and L. Lian, in *Advances in Metal and Semiconductor Clusters*, Vol. 2, edited by M. A. Duncan (JAI, Greenwich, 1994), pp. 1–39.
[3] P. B. Armentrout, J. B. Griffin, and J. Conceição, in *Progress in Physics of Clusters*, edited by G. N. Chuev, V. D. Lakhno, and A. P. Nefedov (World Scientific, Singapore, 1999), pp 198–225.
[4] J. Xu, M. T. Rodgers, J. B. Griffin, and P. B. Armentrout, J. Chem. Phys. **108**, 9339 (1998).
[5] R. Liyanage, J. Conceição, and P. B. Armentrout, J. Chem. Phys. **116**, 936 (2002).
[6] J. B. Griffin and P. B. Armentrout, J. Chem. Phys. **108**, 8062 (1998).
[7] J. B. Griffin and P. B. Armentrout, J. Chem. Phys. **108**, 8075 (1998).
[8] J. Conceição, R. Liyanage, and P. B. Armentrout, Chem. Phys. **262**, 115 (2000).
[9] J. B. Griffin and P. B. Armentrout, J. Chem. Phys. **106**, 4448 (1997).
[10] J. B. Griffin and P. B. Armentrout, J. Chem. Phys. **107**, 5345 (1997).
[11] J. Conceição, S. K. Loh, L. Lian, and P. B. Armentrout, J. Chem. Phys. **104**, 3976 (1996).
[12] F. Liu, R. Liyanage, and P. B. Armentrout, J. Chem. Phys. **117**, 132 (2002).
[13] D. Vardhan, R. Liyanage, and P. B. Armentrout, J. Chem. Phys. (to be published).
[14] P. Schnabel, M. P. Irion, and K. G. Weil, J. Phys. Chem. **95**, 9688 (1991).
[15] M. P. Irion and P. Schnabel, J. Phys. Chem. **95**, 10596 (1991).
[16] P. Schnabel and M. P. Irion, Ber. Bunsenges. Phys. Chem. **96**, 1101 (1992).
[17] K. O. Fossan and E. Uggerud, J. Am. Chem. Soc. (to be published).
[18] G. Ertl, *Catalysis: Science and Technology*, **4**, edited by J. R. Anderson and M. Boudart (Springer, Berlin, 1983); *ibid.* Catal. Rev. - Sci. Eng. **21**, 201 (1980); *ibid. Catalytic Ammonia Synthesis*, edited by J. R. Jennings (Plenum, New York, 1991), p. 109; M. Grunze, F. Boszo, G. Ertl, and M. Weiss, Appl. Surf. Sci. **1**, 241 (1978).
[19] S. K. Loh, D. A. Hales, L. Lian, and P. B. Armentrout, J. Chem. Phys. **90**, 5466 (1989).
[20] T. G. Deitz, M. A. Duncan, D. E. Powers, and R. E. Smalley, J. Chem. Phys. **74**, 6511 (1981).
[21] S. K. Loh, D. A. Hales, and P. B. Armentrout, Chem. Phys. Lett. **129**, 527 (1986).
[22] E. Teloy and D. Gerlich, Chem. Phys. **4**, 417 (1974); D. Gerlich, Adv. Chem. Phys. **82**, 1 (1992).
[23] N. R. Daly, Rev. Sci. Instrum. **31**, 264 (1959).
[24] K. M. Ervin and P. B. Armentrout, J. Chem. Phys. **83**, 166 (1985).
[25] L. Lian, C.-X. Su, and P. B. Armentrout, J. Chem. Phys. **97**, 4072 (1992).
[26] T. Su, J. Chem. Phys. **100**, 4703 (1994).
[27] E. W. Rothe and R. B. Bernstein, J. Chem. Phys. **31**, 1619 (1959).
[28] S. K. Loh, E. R. Fisher, L. Lian, R. H. Schultz, and P. B. Armentrout, J. Phys. Chem. **93**, 3159 (1989).
[29] R. Liyanage and P. B. Armentrout (unpublished).
[30] D. Walter and P. B. Armentrout, J. Am. Chem. Soc. **120**, 3176 (1998).
[31] N. Aristov and P. B. Armentrout, J. Phys. Chem. **91**, 6178 (1987).
[32] L. S. Sunderlin and P. B. Armentrout, J. Phys. Chem. **92**, 1209 (1988).
[33] R. H. Schultz, J. L. Elkind, and P. B. Armentrout, J. Am. Chem. Soc. **110**, 411 (1988).
[34] M. T. Rodgers, K. M. Ervin, and P. B. Armentrout, J. Chem. Phys. **106**, 4499 (1997).
[35] R. H. Schultz, K. C. Crellin, and P. B. Armentrout, J. Am. Chem. Soc. **113**, 8590 (1991).
[36] F. A. Khan, D. E. Clemmer, R. H. Schultz, and P. B. Armentrout, J. Phys. Chem. **97**, 7978 (1993).
[37] T. Beyer and D. F. Swinehart, Commun. Assoc. Computing Machinery **16**, 379 (1973); S. E. Stein and B. S. Rabinovitch, J. Chem. Phys. **58**, 2438 (1973); *ibid.* Chem. Phys. Lett. **49**, 183 (1977).
[38] R. G. Gilbert and S. C. Smith, *Theory of Unimolecular and Recombination Reactions* (Blackwell Scientific, Oxford, 1990).
[39] A. A. Shvartsburg, K. M. Ervin, and J. H. Frederick, J. Chem. Phys. **104**, 8458 (1996).
[40] D. G. Truhlar, B. C. Garrett, and S. J. Klippenstein, J. Phys. Chem. **100**, 12771 (1996).
[41] K. A. Holbrook, M. J. Pilling, and S. H. Robertson, *Unimolecular Reactions*, 2nd ed. (Wiley, New York, 1996).
[42] See EPAPS Document No. E-JCPSA6-119-010341 for 7 figures, 11 tables, and an explanation of the choices for molecular constants used in the data analysis. A direct link to this document may be found in the online article's HTML reference section. The document may also be reached via the EPAPS homepage (http://www.aip.org/pubservs/epaps.html) or from ftp.aip.org in the directory /epaps/. See the EPAPS homepage for more information.
[43] R. Liyanage, X.-G. Zhang, and P. B. Armentrout, J. Chem. Phys. **115**, 9747 (2001).
[44] P. B. Armentrout and B. L. Kickel, in *Organometallic Ion Chemistry*,

edited by B. S. Freiser (Kluwer, Dordrecht, 1996), pp. 1–45.
[45] R. H. Schultz and P. B. Armentrout, J. Chem. Phys. **94**, 2262 (1991).
[46] D. E. Clemmer, L. S. Sunderlin, and P. B. Armentrout, J. Phys. Chem. **94**, 3008 (1989).
[47] M. T. Rodgers and P. B. Armentrout, J. Chem. Phys. **109**, 1787 (1998).
[48] E. K. Parks and S. J. Riley, J. Chem. Phys. **99**, 5898 (1993).
[49] Zh. A. Evdokimova and N. Kh. Valitov, Zh. Prikl. Khim. (S.-Peterburg) **58**, 2121 (1985) (In Russian).
[50] S. W. Buckner and B. S. Freiser, J. Am. Chem. Soc. **109**, 4715 (1987).
[51] S. W. Buckner, J. R. Gord, and B. S. Freiser, J. Am. Chem. Soc. **110**, 6606 (1988).
[52] M. Brönstrup, I. Kretzschmar, D. Schröder, and H. Schwarz, Helv. Chim. Acta **81**, 2348 (1998).
[53] A. D. Becke, J. Chem. Phys. **98**, 5648 (1993).
[54] C. Lee, W. Yang, and R. G. Parr, Phys. Rev. B **37**, 785 (1988).
[55] P. J. Stephens, F. J. Devlin, C. F. Chabalowski, and M. J. Frisch, J. Phys. Chem. **98**, 11623 (1994).
[56] M. J. Frisch, G. W. Trucks, H. B. Schlegel *et al.*, , Revision A.7 (Gaussian, Inc., Pittsburgh, PA, 1998).
[57] J. B. Foresman and Æ. Frisch, *Exploring Chemistry with Electronic Structure Methods*, 2nd ed. (Gaussian, Pittsburgh, 1996).
[58] D. Brennan, D. O. Hayward, and B. M. W. Tradnell, Proc. R. Soc. London, Ser. A **256**, 81 (1960); J. Bragg and F. C. Tomkins, Trans. Faraday Soc. **51**, 1071 (1955); G. Wedler, Z. Phys. Chem. (Leipzig) **27**, 388 (1961).
[59] F. Boszo, G. Ertl, M. Grunze, and M. Weiss, Appl. Surf. Sci. **1**, 103 (1977).
[60] F. Boszo, G. Ertl, and M. Weiss, J. Catal. **50**, 519 (1977).
[61] J. B. Benziger, in *Metal-Surface Reaction Energetics*, edited by E. Shustorovich (VCH, New York, 1991), pp. 53–107.
[62] F. Boszo, G. Ertl, M. Grunze, and M. Weiss, J. Catal. **48**, 18 (1977).
[63] J. J. Mortensen, M. V. Ganduglia-Pirovano, L. B. Hansen, B. Hammer, P. Stoltze, and J. K. Nørskov, Surf. Sci. **422**, 8 (1999).